REVIEW

Organic Stereochemistry

Part 5[1])

Stereoselectivity in Molecular and Clinical Pharmacology

by **Bernard Testa***[a]), **Giulio Vistoli**[b]), **Alessandro Pedretti**[b]), and **John Caldwell**[c])

[a]) Department of Pharmacy, Lausanne University Hospital (CHUV), Rue du Bugnon, CH-1011 Lausanne (e-mail: Bernard.Testa@chuv.ch)

[b]) Dipartimento di Scienze Farmaceutiche 'Pietro Pratesi', Facoltà di Farmacia, Università degli Studi di Milano, Via Mangiagalli, 25, I-20133 Milano

[c]) Faculty of Health and Life Sciences, University of Liverpool, Liverpool L69 7ZX, UK

All stereogenic elements having been discussed and illustrated in *Parts 2–4*, the road is open to change focus. Our *Series on Organic Stereochemistry* now moves from fundamental stereochemical principles to biomedicinal applications. Due consideration is now given in *Parts 5* and *6* to the *pharmacological significance* of configurational and conformational factors, respectively. This will be followed by illustrations taken from *biochemistry* (endobiotic metabolism) and mainly *xenobiotic metabolism*, specifically with respect to substrate stereoselectivity (*Part 7*) and product stereoselectivity (*Part 8*).

The present *Part* covers various pharmacological fields in which stereochemistry plays a major role [1–10]. Thus, we shall begin with the phenomenon commonly known as '*chiral recognition*', namely the molecular mechanisms by which a chiral molecule, in our case a target biomacromolecule, selectively interacts with a medicinal ligand, which may be an agonist, activator, antagonist, substrate, or inhibitor of the key function of the target in question. This will be followed by a computational example, namely an original molecular modeling (MM) and molecular dynamics (MD) study of the interaction of hyoscyamine enantiomers with three cholinergic muscarinic receptors. Various pharmacological aspects and implications of stereoselectivity in drug action will then be discussed, followed, in the last section, with the role played by configurational factors in drug disposition, specifically absorption, distribution, and excretion.

---

[1]) For the other *Parts*, see *Helv. Chim. Acta* **2013**, *96*, 1–3.

Fig. 5.1. The *content of this Part* is summarized here and follows the sequence outlined in the *Introduction* above. Our first encounter with stereoselective recognition processes will occur with *conceptual models*, that is to say graphical representations that encapsulate the necessary (assumed to be sufficient) conditions for enantioselective recognition (so-called 'chiral recognition' [11]) to occur between two molecules. A more recent – and much more informative – way of depicting these recognition processes involves new computational tools such as *molecular modeling* and *molecular dynamics*, as exemplified below with the enantiomers of hyoscyamine in their interactions with muscarinic receptors.

Stereoselectivity in pharmacodynamic processes is considered next, involving the presentation and illustration of rationalizations such as the influence of optical purity on enantioselectivity, *Pfeiffer*'s rule and eudismic analysis, and differential stereoselectivity in the recognition and activation steps at biologically relevant targets. Finally, in the remainder of this *Part* examples of stereoselectivity in the pharmacokinetic processes of (drug) *absorption*, *distribution*, and *excretion* are presented.

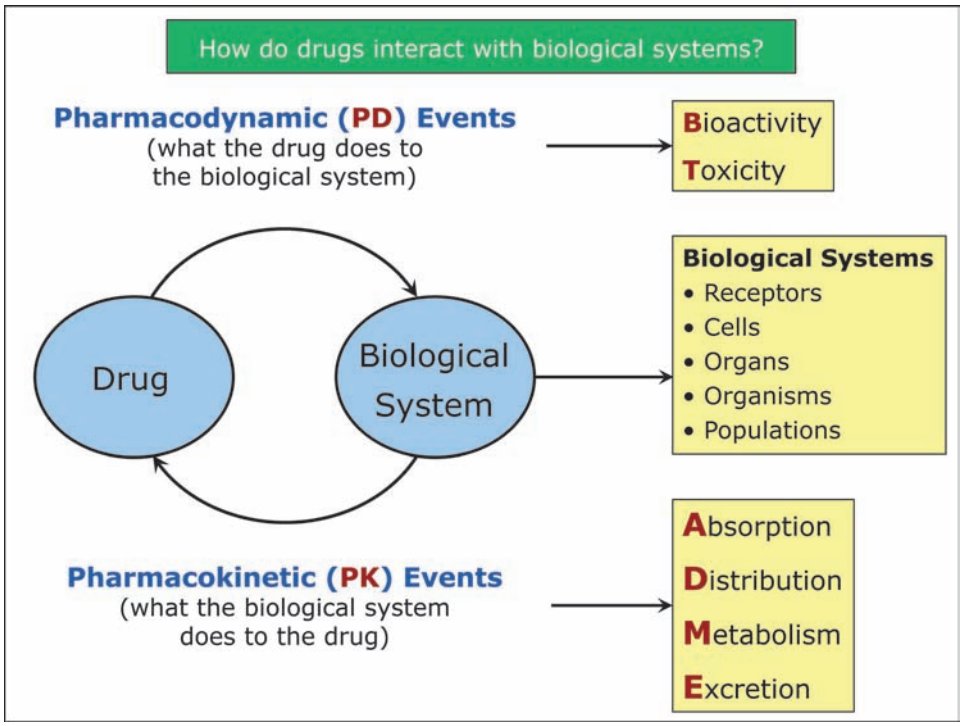

Fig. 5.2. Before beginning with the proper topic of this *Part*, we recall in schematic form the two aspects of the interactions between a drug (or any xenobiotic) and a biological system [12]. Note that '*biological systems*' are defined very broadly and include functional proteins (*e.g.*, receptors), monocellular organisms and cells isolated from multicellular organisms, isolated tissues and organs, multicellular organisms and even populations of individuals, be they uni- or multicellular. As for the *interactions* between a drug and a biological system, they may be expressed simply as '*what the compound does to the biosystem*' and '*what the biosystem does to the compound*'.

In pharmacology, one speaks of '*pharmacodynamic effects*' to indicate what a drug does to the body, and '*pharmacokinetic effects*' to indicate what the body does to the drug. But one must appreciate that these two aspects of the behavior of xenobiotics are inextricably interdependent. *Absorption*, *distribution*, and *excretion* (ADE) will obviously have a decisive influence on the intensity and duration of pharmacodynamic effects, whereas *biotransformation* (*metabolism*) will generate metabolites which may be inactive or may have distinct pharmacodynamic effects of their own, be they exerted at the same of different targets as the parent drug. Furthermore, due to its own pharmacodynamic effects, a compound may affect the state of the organism (*e.g.*, changes in hemodynamic flow and enzyme activities) and hence its capacity to handle xenobiotics.

The *Figure* is meant to help readers understand the classification we have adopted, with pharmacodynamic processes then ADE discussed in the present *Part* and in *Part 6*, whereas endobiotic and xenobiotic metabolisms will be considered in *Parts 7* and *8*.

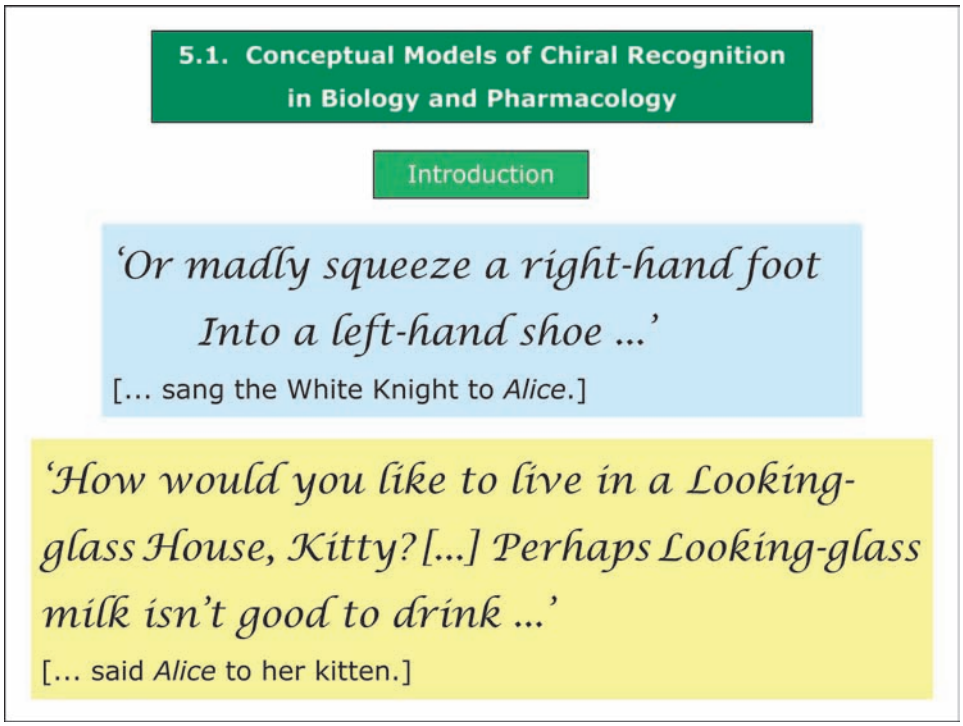

Fig. 5.3. Perhaps the first report of enantioselectivity in a biological effect is the observation by *Piutti* in 1886 that the two enantiomers of asparagine differ in taste, since the (+)-form was sweet while the (−)-form was insipid [13]. Since then, numerous organoleptic differences between enantiomers have been discovered [14]. Around the end of the 19th century and the beginning of the 20th, a number of studies were carried out on differences in the biological effects of enantiomers, but it seems that the first clear proofs were provided by *Cushny* [15].

Not seldom, the artist's intuition anticipates scientific discoveries, and enantioselectivity is no exception. Indeed, *Charles Lutwidge Dodgson*, better known by his *nom de plume Lewis Carroll*, had two amazing statements to offer in his classic '*Through the Looking-Glass and What Alice Found There*' published in 1871 [16]. The first quotation in the *Figure* encapsulates *chiral recognition* in a vivid and lasting way. The second quotation applies to enantioselectivity at a macroscopic biological level, implying that enantiomers (here a type of food and its mirror-image opposite) may have different effects in the body.

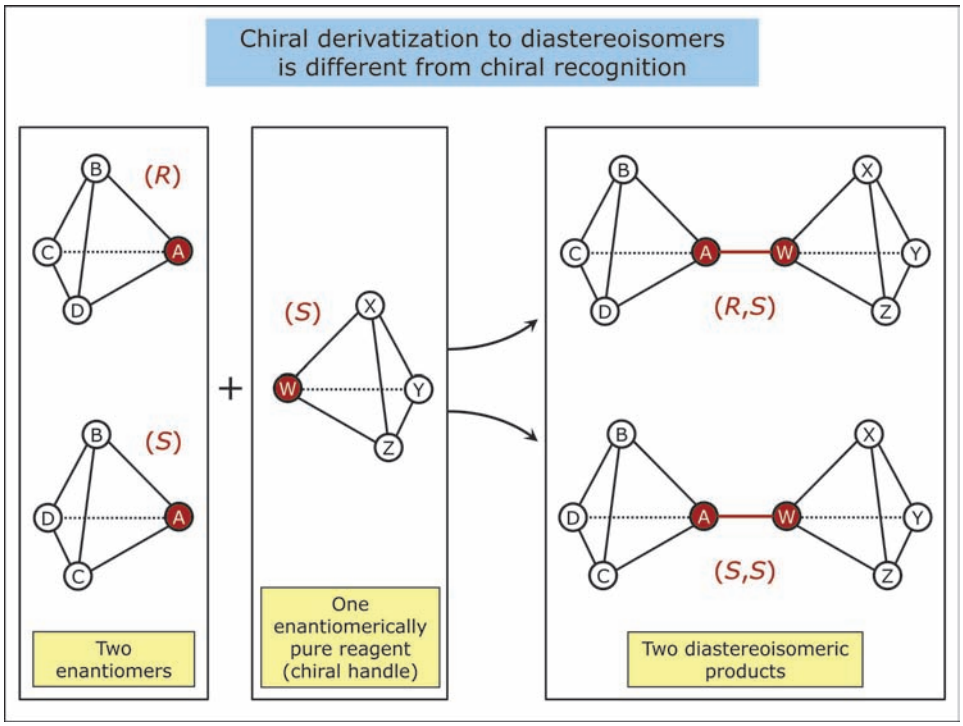

Fig. 5.4. Before discussing graphic models of chiral recognition, we highlight *what the latter is not*, namely *chiral derivatization* with an enantiomerically pure reagent. Since enantiomers have identical chemical and physical properties in an achiral context (see *Part 1*), their discrimination or physical separation necessitates a '*chiral handle*'. In enantioselective chromatography, for example, this may be an enantiomerically pure derivatization reagent forming a covalent bond with the analyte, as illustrated here with two enantiomeric analytes. The functional groups A (in the analytes) and W (in the reagent) are highlighted in red. Their coupling forms *two diastereoisomeric products* which, by their very nature, have different physicochemical properties allowing their separation [17][18].

Importantly, there is *no discrimination in this process between the two enantiomeric analytes*, since both are expected to react to completion with the reagent. This is the opposite of what happens in living systems where the discrimination step between enantiomers (the *chiral recognition step*) is often *reversible*, implying *differential affinity to and/or interaction with the binding site*. The same is true for example in liquid chromatography on chiral columns, a point outside our argument.

Living organisms, like chiral columns, are enantiomerically pure at the molecular level. Indeed, only L-amino acids are encoded in proteins, whereas most sugars have the D-configuration. In addition, helicity in proteins is preferably right-handed. In consequence, hormones, enzymes, receptors, transporters, immunoglobulins, *etc.*, are all chiral and enantiomerically pure. Enantiomers will, therefore, interact differently with them. This is the *basis of chiral recognition* in pharmacodynamic and pharmacokinetic processes, as illustrated throughout this *Part* and the following ones.

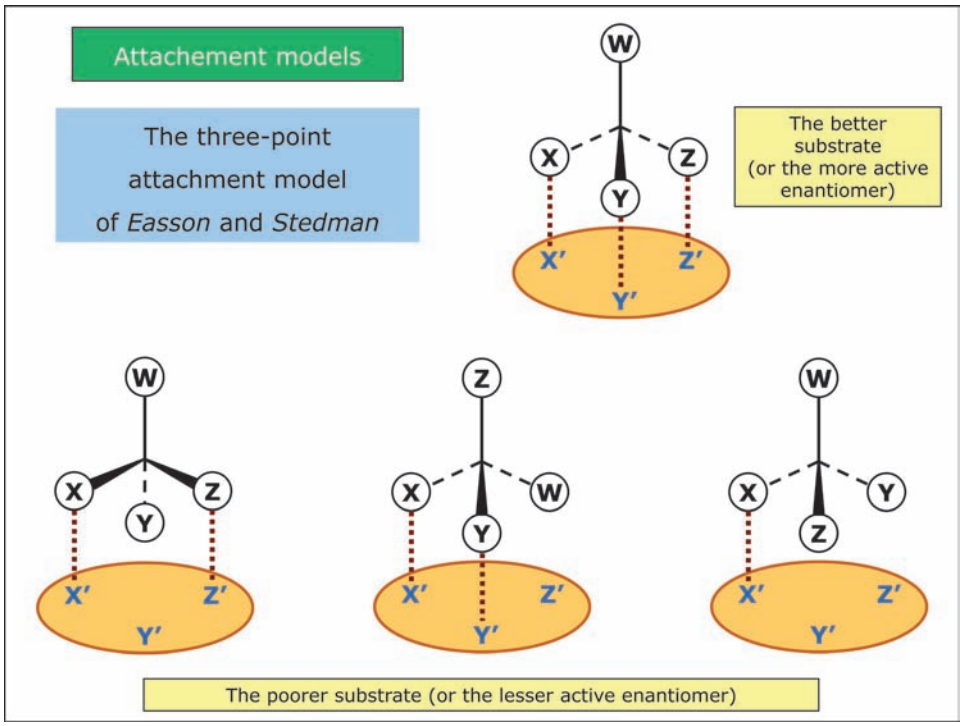

Fig. 5.5. Our current understanding of biological enantioselectivity owes much to the attachment model of *Easson* and *Stedman* [19]. In comparing the biological behavior of enantiomers containing a single center of asymmetry, they proposed a *three-point attachment model* to account for the observed selectivities. This model postulates *three binding sites* in the receptor (X′, Y′, and Z′) to which *three complementary (pharmacophoric) groups* (X, Y, and Z) correspond in the drug molecule. In the more active enantiomer (the *eutomer*, see later), the three pharmacophoric groups can be positioned so as to simultaneously interact with the three receptor sites. In contrast, the less active enantiomer (the *distomer*, see later) can bind only *via* one or two out of its three complementary groups, hence its weaker affinity.

An obvious feature of the current model is that it considers only *attractive interactions* between receptors and eutomers. But is current knowledge compatible with chiral recognition being based solely on attractive interactions? As clearly demonstrated by *Fersht* [20], *unfavorable (repulsive) interactions* can also be an important determinant of specificity. Such repulsive interactions may be steric or electrostatic in nature, implying that one site on the receptor may, for example, be a zone of *steric hindrance*. *Meyer* and *Rais* have published vivid pictorial descriptions of chiral three-point recognition, including the case where one interaction is repulsive [21].

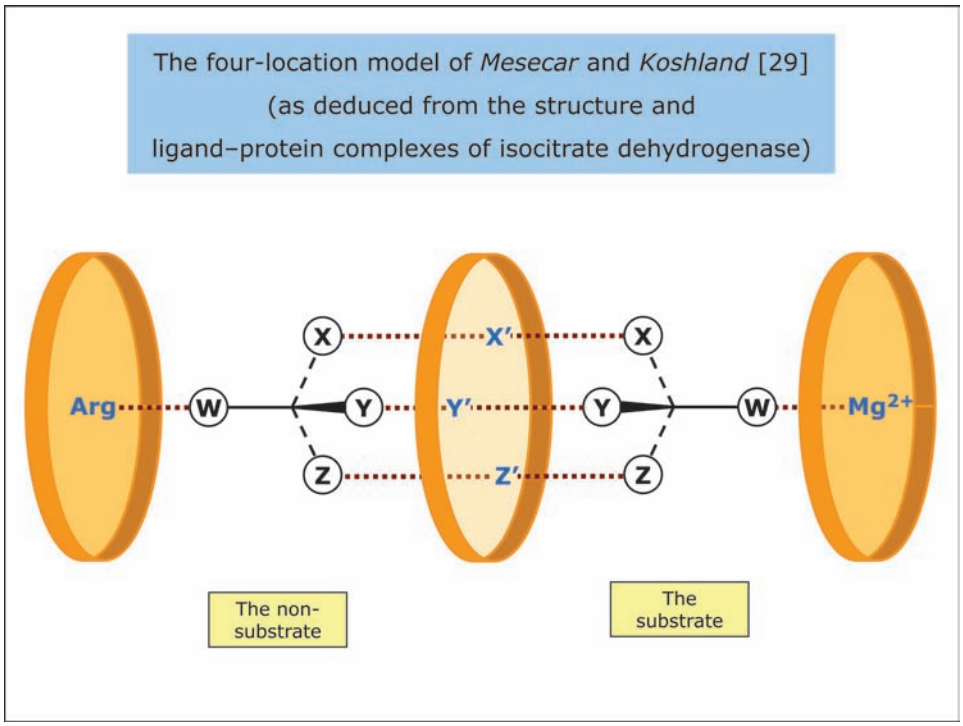

Fig. 5.6. Several years ago, there were debates about the general validity of a three-point attachment model [22–26], with analysts, quantum chemists, and biochemists adopting different viewpoints. A valuable argument is, for example, that the standard three-point model involves three coplanar contact points, while the minimal requirement may in some cases be four nonplanar sites [27–29]. This was observed in a crystallographic study of *isocitrate dehydrogenase*, showing that three of its binding sites (X′, Y′, and Z′) are located on the internal face of a cavity (here depicted as a ring). As a result, these three sites alone would allow both enantiomers of the substrate to bind with similar affinity, with the fourth group in the substrate (W) pointing in either direction. Enantioselectivity is achieved by a fourth site which proved to be *Arg119* in the metal-free, non-functional enzyme, and Mg^{2+} in the *magnesium-containig functional enzyme* [29]. Only the non-substrate (−)-(1*S*,2*R*)-isocitric acid (L-isocitric acid) was found to bind to the metal-free enzyme, whereas only the physiological substrate (+)-(1*R*,2*S*)-isocitric acid (D-isocitric acid) did bind to the Mg^{2+}-containing enzyme, a reaction we will detail in *Part 7*. In other words, enantioselectivity was not seen in the binding step, since the two enantiomers of isocitric acid were bound, but instead at the catalytic step.

In such a *four-location model*, there may be four attachment sites, or three attachment sites plus one direction. The latter case is in fact the model of *Easson* and *Stedman* which must, therefore, be considered as a particular case of the more general four-location model.

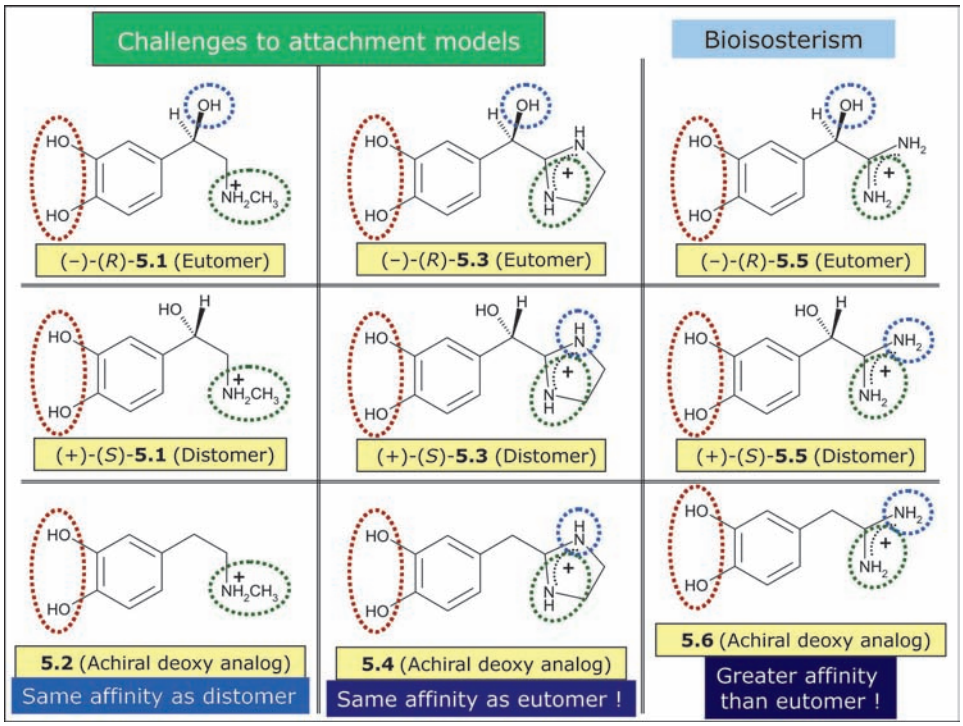

Fig. 5.7. The *Easson–Stedman* model was challenged with *adrenaline* (**5.1**) and its *catecholimidazoline* and *catecholamidine* analogs, **5.3** and **5.5**, respectively [30][31]. In each series, the *hydroxylated enantiomers*, **5.1**, **5.3**, and **5.5**, followed the order of affinity to the α-adrenoceptor predicted by the model, namely $(R) > (S)$. However, and in contrast to the prediction, the *deoxy analogs*, **5.2**, **5.4**, and **5.6**, had equal (catecholimidazolines) or greater (catecholamidines) affinities than the respective eutomers of their hydroxy analogs! These findings were interpreted to mean that the *Easson–Stedman* model cannot be extended to catecholimidazolines and catecholamidines. However, such an interpretation resulted from a static and too literal understanding of the model. This is explained by considering the *three pharmacophoric groups* in eutomers, namely the catechol function (red ovals), the cationic head (green ovals), and the OH group (blue circles). In the protonated imidazolinyl and amidinyl moieties of the hydroxylated compounds, **5.3** and **5.5**, respectively, one of the NH/NH_2 groups fulfills the role of the amino group in protonated adrenaline. In the deoxy analogs **5.4** and **5.6**, however, the other NH/NH_2 group is suitably located to replace the missing benzylic OH group as an H-bond donor to the receptor. The model thus retains its validity if *bioisosterism* is taken into account, namely the replacement of a functional moiety with one different in chemical composition yet comparable in stereoelectronic terms, *i.e.*, an *isosteric group* [32]. When this stereoelectronic analogy satisfies a biological receptor, one speaks of *bioisosterism*.

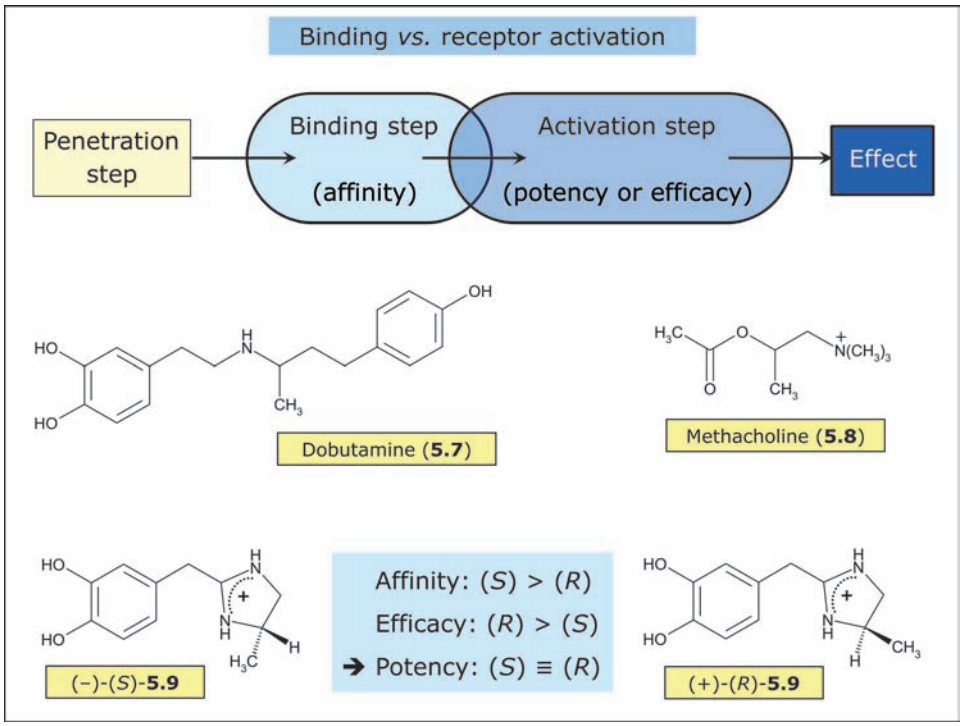

Fig. 5.8. *Easson* and *Stedman* started from the implicit assumption that the enantioselectivity of receptors and enzymes is due to *differential affinity* (*i.e.*, *binding*), and they explicitly and repeatedly stated that their model is one of *attachment* [19]. Whether differential binding is the sole mechanism of chiral recognition in biochemical pharmacology is challenged here. From a general viewpoint, the interaction of a xenobiotic, and more generally of any chemical compound, with a *macromolecular 'machine'* (*e.g.*, receptor, enzyme, or transporter) begins by reaching the target (penetration) and ends with an effect. What happens in between is relevant here and can be broken down into two steps [33–35].

As shown, these are *a*) a *binding step* (*recognition*) measured as *affinity* and involving the binding (complex formation) to the macromolecular machine, and *b*) an *activation step* resulting in the functional response of the macromolecular machine. This response is measured in pharmacology as *potency* (*i.e.*, the concentration of a drug necessary to obtain a given response, generally 50% of maximal response) or as *efficacy* of the agonist–receptor complex (*i.e.*, the percentage of the receptor population to be occupied to elicit 50% of its maximal response).

These two steps are conceptual and partly overlapping, and as such they have the utility and limitation of schematic perceptions. It is known, however, that both the binding and the activation steps, either alone or together, can contribute to chiral recognition in pharmacodynamic and pharmacokinetic processes. A few examples are presented below to demonstrate that chiral recognition does not need to be restricted to the binding step, but can also occur at the activation step. Thus, the two enantiomers

of *dobutamine* (**5.7**) displayed identical affinities to α_1-*adrenoceptors* in rat aorta (its effects on β-adrenoceptors are not under discussion), but only the (−)-(*S*)-enantiomer behaved as an agonist by being able to activate the receptors. The (+)-(*R*)-enantiomer lacked agonist activity and was a competitive α_1-adrenoceptor blocker [3][36][37]. In this example, chiral recognition is thus limited to the activation step.

A more complex situation was encountered in the activation of muscarinic presynaptic receptors by the enantiomers of *methacholine* (**5.8**), both of which acted as full agonists [3][38]. While the ratio of *affinities* was 180, the ratio of *potencies* was 650. Thus, not only did (+)-(*S*)-methacholine (the eutomer) show a higher affinity, it also had to occupy fewer receptors than its distomer to elicit 50% of the maximal response. In other words, the high eudismic ratio in potency resulted from synergistic chiral recognition involving both the binding and activation steps.

The enantiomeric pairs of catecholamines **5.1**, **5.3**, and **5.5** were discussed in *Fig. 5.6* in terms of receptor affinity, but they also displayed differences in potency [30]. Further model compounds were presented in this study, for example, an analog C-*methylated on the imidazoline ring* (**5.9**). The receptor affinities of its enantiomers were somewhat lower than those of the non-*C*-methylated parent, **5.4**, but a clear difference in *affinity* was seen between the enantiomers, which was greater for (*S*)-**5.9**. In contrast, (*R*)-**5.9** showed a higher *efficacy* which compensated for its lower affinity. As a result, the two enantiomers had identical *potencies*. In other words, the (*S*)-enantiomer had to occupy more receptors than its (*R*)-enantiomer to elicit a 50% maximal response.

To summarize, the selected examples discussed here demonstrate that *stereoselectivity in pharmacodynamic processes can result from either or both of the binding and activation steps*. While static and schematic attachment models have their advantages, they also have severe limitations and, if not lucidly used, may lead to a damaging misunderstanding of drug–receptor interactions. In particular, attachment models cannot offer insight on *ligand–receptor induced fit* and on *further conformational rearrangements* leading to an effect (agonistic, antagonistic, catalytic, or inhibitory). This is where *molecular modeling* and *molecular dynamics* have major roles to play.

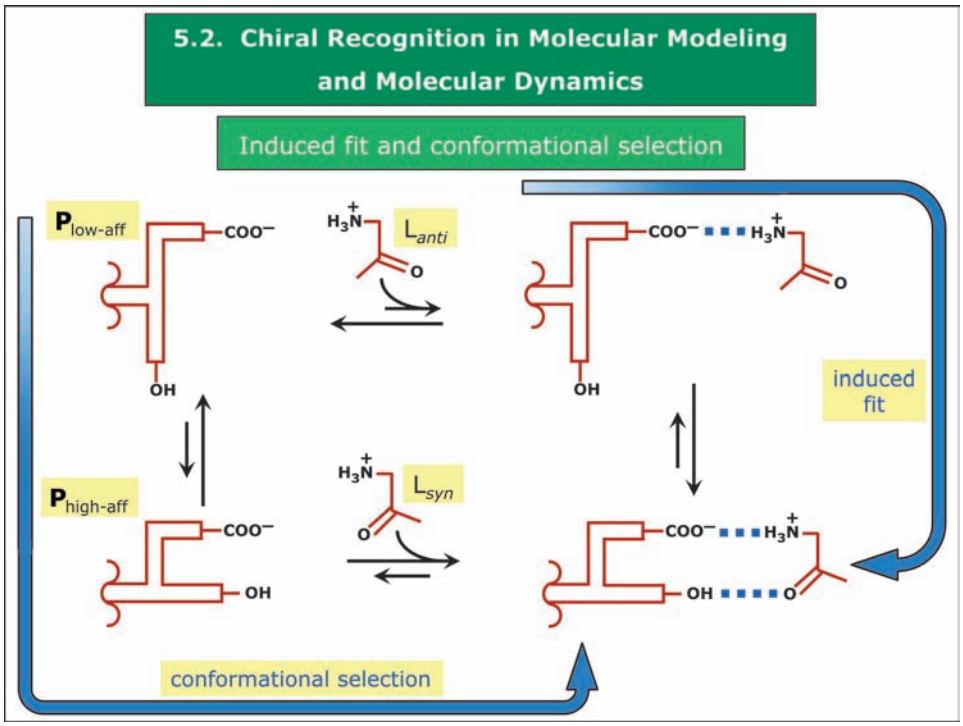

Fig. 5.9. The above *Figures* have illustrated various popular models of enantioselective recognition in biochemistry and pharmacology, also pointing to some refinements such as a need to consider *bioisosterism* and *mutual adaptability*. Here, we examine the latter aspect and illustrate it in some detail. It is indeed universally accepted that the '*Lock-and-Key Model*' proposed in 1890 by *Emil Fischer* [39] is far too limited, as it does not account for the critical role played by the flexibility of both ligand and target, and their mutual adaptability in increasing affinity and, when relevant, efficacy.

Two main models have been proposed to depict this process of mutal adaptability in biochemistry and pharmacology, namely the '*induced-fit model*' [40–44] and '*conformational selection*' [45]. While the two models were seen by some to be mutually incompatible, many recent investigations have demonstrated their complementary character and consider them as extremes in a continuum of possibilities [46–54]. In the schematic representation presented here (inspired by [48][49]), the target protein (**P**) is assumed to exist in two conformational states, one with low affinity for the ligand, the other with high affinity. Similarly, the ligand (**L**) is assumed to be in a *syn–anti* conformational equilibrium. In the *induced-fit process*, ligand binding to $\mathbf{P}_{\text{low-aff}}$ (*e.g.*, through a ionic bond) generates a complex of sufficient stability to allow subsequent conformational rearrangement of both protein and ligand to reach an optimal fit and a low-energy level. In the *conformational selection model*, the ligand binds directly to $\mathbf{P}_{\text{high-aff}}$ and thereby shifts the conformational equilibrium of the protein. It seems clear from this *Figure* that either or both processes can operate depending on the relative equilibrium constants.

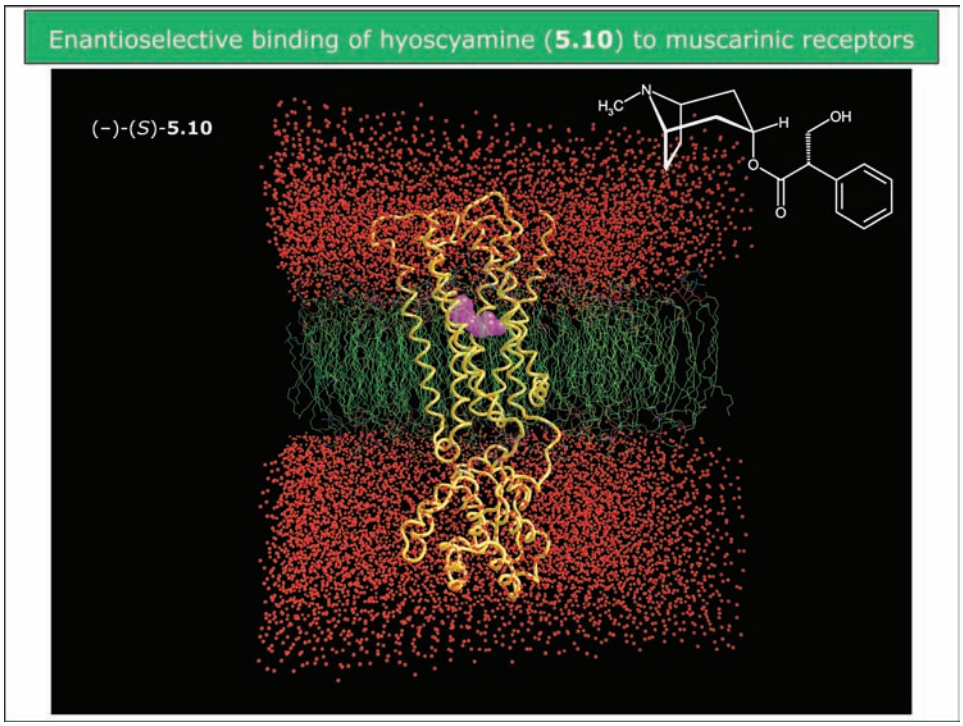

Fig. 5.10. Following this summary of *induced fit* and *conformational selection*, let us now come one step nearer to physical reality with *Molecular Modeling* (MM) and *Molecular Dynamics* (MD), two computational tools which have made significant contributions to our understanding of stereoselective ligand–target recognition [55]. To this end, we examine in molecular detail the complexes formed by the anticholinergic *hyoscyamine* (**5.10**) *enantiomers* with three human *muscarinic receptors* (*i.e.*, hmAChR2, hmAChR3, and hmAChR5). The 3D structures for the hmAChR2 and hmAChR3 subtypes were recently resolved [56], while that of hmAChR5 was generated by homology techniques using the previous one as the multiple templates [57]. Hyoscyamine (**5.10**) was chosen on the basis of its medicinal relevance [58][59] and marked stereoselectivity of action, the natural (*S*)-enantiomer being the eutomer [60]. Also, docking studies with hyoscyamine isomers binding to human muscarinic receptors have never been reported.

The two hyoscyamine isomers were simulated in their protonated form, which is believed to be involved in receptor binding[2]). As illustrated here, the putative complexes formed by the *protein* (the light yellow ribbon model) and the *ligand* (the central, bright-pink molecule) were inserted into a *membrane model* composed of a bilayer of phosphatidylcholine (POPC) molecules (the green threads) and surrounded by two bands of *H_2O molecules* (red dots). After a preliminary minimization to optimize the relative position of membrane molecules, the systems underwent 5-ns molecular dynamics (MD) runs. These simulations were conducted using the same computational procedures described in [57].

---

[2]) The conformational behavior of the compounds was investigated by a clustered Monte-Carlo procedure. For each ligand, the lowest-energy structure was then used in the docking simulations. The two resolved structures were retrieved from PDB (Id: 3UON for hmAChR2 and 4DAJ for hmAChR3), and after adding H-atoms they were minimized keeping fixed the backbone atoms to preserve the experimental folding. The structure of hmAChR5 was modeled by homology techniques using Modeller9.10 and the two resolved structures as multiple templates. Again, the completed model was minimized keeping fixed the backbone atoms to preserve the predicted folding. Docking simulations were then performed by GriDock, a parallel tool based on the AutoDock4.0 engine. For the two resolved receptors, the grid boxes were set to include all residues within a 15-Å radius sphere around the bound inhibitor, while the grid box of hmAChR5 was set to include all residues within a 15-Å radius sphere around Asp110, thus comprising the entire binding site. The resolution of the grid was $60 \times 60 \times 60$ points with a grid spacing of *ca.* 0.50 Å. For the docking simulations, the flexible bonds of the ligand were automatically recognized by GriDock and left free to rotate so as to account for ligand flexibility within the binding cavity. The enantiomeric ligands were docked with the *Lamarckian* algorithm as implemented in AutoDock. The genetic-based algorithm ran 30 simulations per substrate with 2,000,000 energy evaluations and a maximum number of generations of 27,000. The crossover rate was increased to 0.8, and the number of individuals in each population to 150. All other parameters were left at the AutoDock default settings. The best complexes were finally minimized to favor the mutual adaptability between ligand and receptor, and the optimized complexes were then used to re-calculate docking scores.

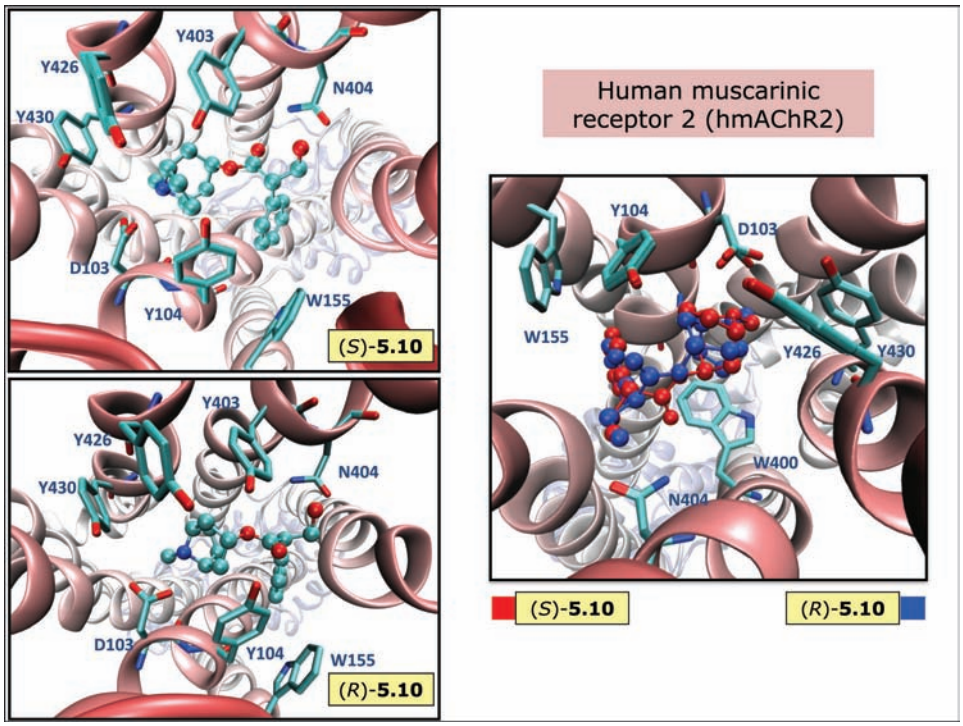

Figs. 5.11 – 5.13. These *Figures* will illustrate the best complexes of hyoscyamine enantiomers binding to the hmAChR2 (*Fig. 5.11*), hmAChR3 (*Fig. 5.12*), and hmAChR5 (*Fig. 5.13*) as computed by the AutoDock program[2]). The relevant docking scores are compiled in *Fig. 5.14*, while a MD study of the stereoselective recognition process for hmAChR2 is presented in *Fig. 5.15.*

The *left side* of the three *Figures* shows the separate, lowest-energy complexes of (*S*)- and (*R*)-hyoscyamine with the receptor. The ligands are represented as ball-and-stick models while the interacting residues are in a simple stick representation, both of them without H-atoms for clarity. The color code of atoms is C cyan, H white, O red, and N blue. The *right side* of the *Figures* shows the superposition of the two individual complexes. For better clarity, the angles of vision of the two separate complexes differ from that of their superposition.

Fig. 5.11 shows the difference between the interaction patterns stabilized by hyoscyamine enantiomers within the *hmAChR2 receptor*. The contacts elicited by the charged amino group are almost identical, namely an *ion pair* with D103 (Asp103), a *reinforced H-bond* with Ser109 (not displayed for clarity), and a set of *charge-transfer interactions* with surrounding tyrosine residues (Y104, Y403, Y426, and Y430), which constitute the characteristic feature of all muscarinic binding sites. Yet again, the phenyl ring elicits *π–π stacking* with W155 (Trp155) and W400 (Trp400) in both complexes. In contrast, the computed complexes mainly differ in the interactions between the polar moieties attached to the stereogenic center and N404 (Asn404). Indeed, both the carbonyl O-atom and the OH group of (*S*)-hyoscyamine form *H-bonds* with N404.

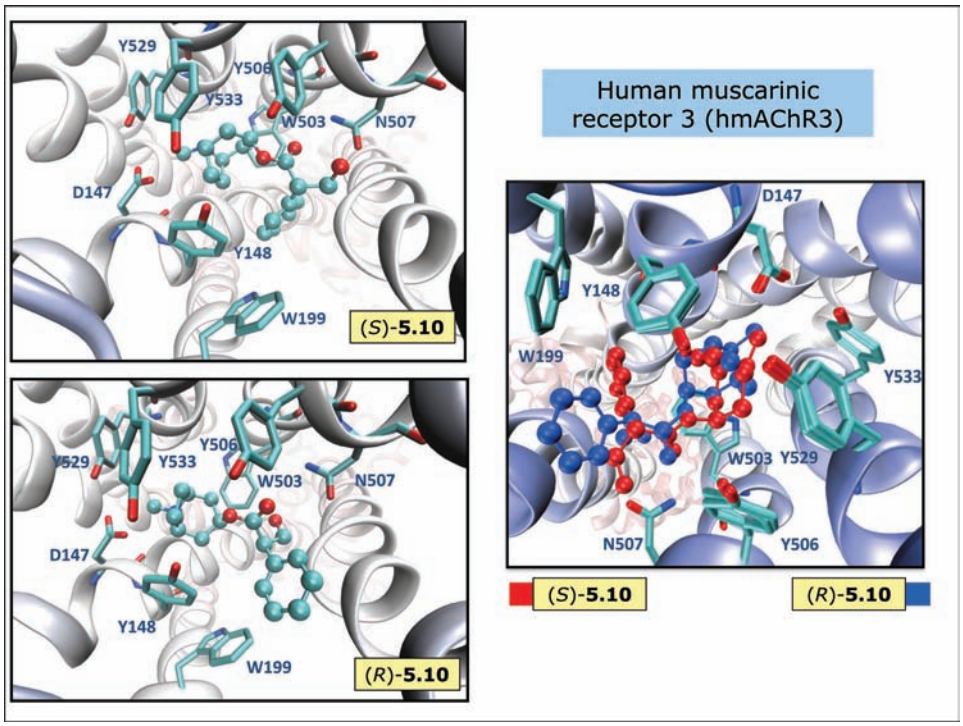

Fig. 5.12.

Conversely, the different spatial arrangement of the carbonyl O-atom of the (*R*)-enantiomer prevents its key interaction with N404 which here retains a weak H-bond with the OH group only.

Coming to the *hmAChR3 receptor* (*Fig. 5.12*), the differences between the complexes formed by (*S*)- and (*R*)-hyoscyamine appear more pronounced than those described for the hmAchR2. Also here, both hyoscyamine enantiomers showed a similar position of the protonated amino group which stabilizes an *ion pair* with D147 (Asp147), a *reinforced H-bond* with Ser151 (not displayed for clarity), and a set of *charge-transfer interactions* with surrounding tyrosine residues (Y148, Y506, Y529, and Y533). The main differences between hyoscyamine enantiomers and with the previous receptor concern the moieties connected to the stereogenic center. Indeed, the two complexes with hmAChR2 mainly differ for the carbonyl arrangement, while showing similar interactions stabilized by the phenyl ring and the OH group. In contrast, the two hyoscyamine enantiomers within the hmAChR3 binding site show almost identical orientations of the carbonyl group which elicit in both complexes a H-bond with N507 (Asn507), while they differ for the arrangement of both the phenyl ring and the OH group. In detail, the OH group of (*S*)-hyoscyamine contacts N507, and its phenyl ring elicits π–π stacking with both W199 (Trp199) and W503 (Trp503), whereas the OH group of (*R*)-hyoscyamine does not approach the N-atom, and the phenyl ring is inserted in a more hindered subcavity where it can contact alkyl side chains only (Leu225 and Val 510; not shown).

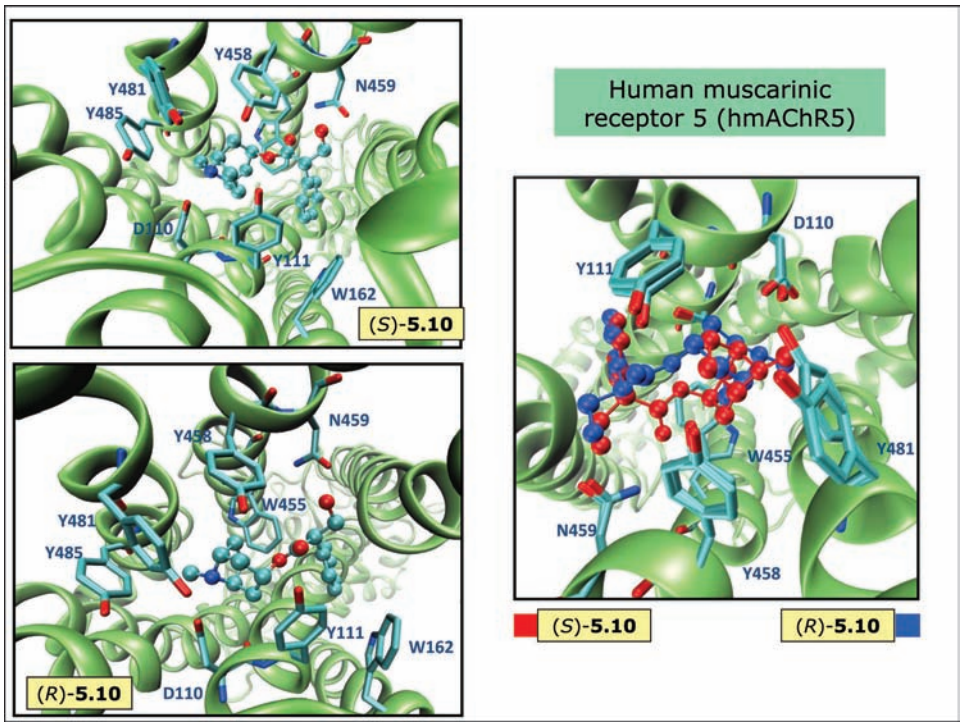

Fig. 5.13.

In the *hmAChR5* binding site (*Fig. 5.13*), the differences between the two complexes are comparable to those observed for hmAChR1. Indeed, the charged ring stabilizes similar contacts in both isomers including an ion pair with D110 (Asp110) and π–cation contacts with tyrosine residues (Y111, Y458, Y481, and Tyr485), while the major difference concerns the arrangement of the C=O O-atom which can form a H-bond with N459 (Asn459) only in the (*S*)-hyoscyamine complex. Notably, the ligand's phenyl ring and the OH group stabilize superimposable interactions in both complexes, namely π–π stacking with W162 (Trp162) and W455 (Trp455), and a H-bond with Asn459, respectively.

Scores of mAChRs complexes with hyoscyamine enantiomers

mAChR	Hyoscyamine enantiomers	Affinity (pK_i values; K_i in M)	Electrostatic energy [kcal/mol]	CHARMM energy [kcal/mol]	Root-mean-square deviation	Mean distance between the phenyl rings in the two complexes
mAChR2	(*S*)	9.48	−35.57	−42.45	1.9 Å	0.5 Å
	(*R*)	8.21	−35.67	−38.77		
mAChR3	(*S*)	9.45	−36.45	−42.33	4.2 Å	6.6 Å
	(*R*)	7.89	−36.82	−36.08		
mAChR5	(*S*)	9.24	−32.56	−41.73	2.2 Å	0.2 Å
	(*R*)	8.17	−32.17	−38.08		

Fig. 5.14. A few data and scores are presented here to summarize some of the key features of the six complexes between hyoscyamine enantiomers and the three muscarinic receptors investigated. The *third column* contains the *experimental* pK_i *values* [60], implying that (*S*)-hyoscyamine has a 10- to 40-fold greater *receptor affinity* than its enantiomer. The *fourth and fifth columns* compare the energy content of the complexes as calculated by the docking algorithm, confirming the greater stability of the (*S*)-enantiomer complexes. In more details, all complexes show comparable, if not similar, electrostatic energy scores, but marked differences in the non-ionic energy scores (as computed by the CHARMM energy which encodes H-bonding, *Van der Waals* interactions, and π–π stacking and apolar contacts), since the two isomers differ in the arrangement of their H-bonding groups and/or phenyl ring in each simulated receptor. Notably, the greatest difference is seen for hmAChR3 where the two isomers differ both in the stabilized H-bonds and in the position of the phenyl ring.

Given that the hmAChR2 is more flexible than the hmAChR3 [56], this factor offers an explanation for the differences observed between the two receptor complexes. Indeed, a more rigid binding site cannot adapt as well as a more flexible one to interact with two enantiomers. While in all muscarinic receptors the dominant ionic bond is constantly conserved, the other moieties assume a completely different arrangement only in the less flexible hmAChR3. Finally, the hmAChR5 shows an intermediate behavior with higher similarity to hmAChR2.

Such considerations are confirmed by the *root-mean-square deviation* (RMSD) values, namely the average deviations in distances between the bound enantiomers, computed from the heavy atoms only (*penultimate column*). The same is true for the *distance between the geometric centers of the phenyl rings* in the bound enantiomers (*last column*), as measured directly in the superimposed complexes (*Figs. 5.11–5.13*). Indeed, the hmAChR3 shows the largest RMSD value, as easily justified by the largest distance between the phenyl rings. The hmAChR2 and hmAchR5 in contrast have low RMSD values which are in line with the very low distances between the phenyl moieties.

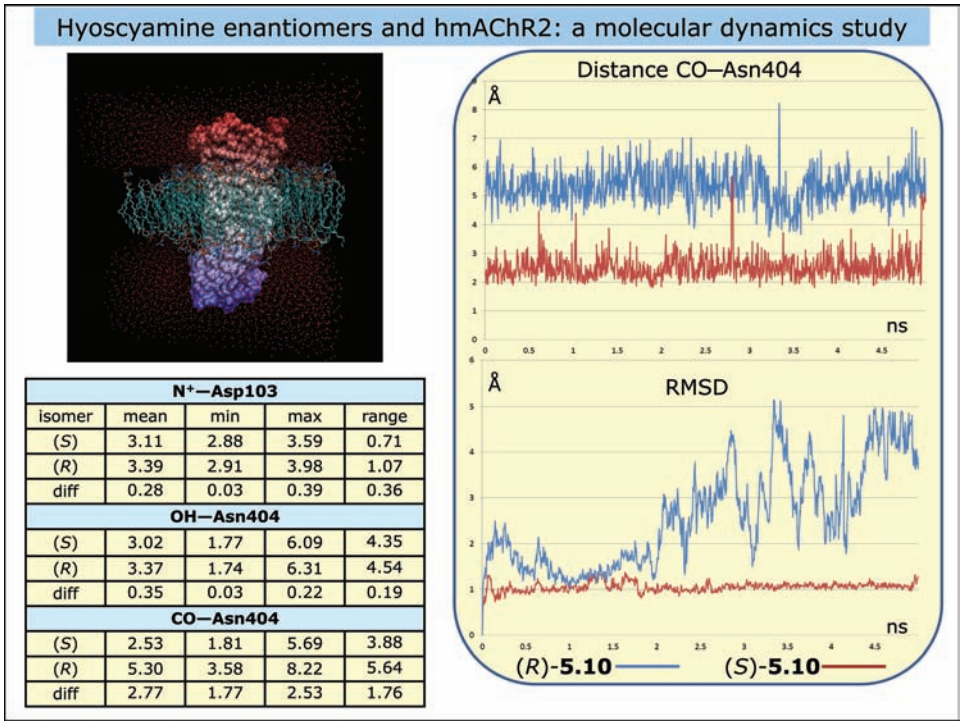

N⁺—Asp103				
isomer	mean	min	max	range
(*S*)	3.11	2.88	3.59	0.71
(*R*)	3.39	2.91	3.98	1.07
diff	0.28	0.03	0.39	0.36
OH—Asn404				
(*S*)	3.02	1.77	6.09	4.35
(*R*)	3.37	1.74	6.31	4.54
diff	0.35	0.03	0.22	0.19
CO—Asn404				
(*S*)	2.53	1.81	5.69	3.88
(*R*)	5.30	3.58	8.22	5.64
diff	2.77	1.77	2.53	1.76

Fig. 5.15. A *Molecular Dynamics* (MD) study was performed to investigate how the differences between the computed hmAChR2 complexes affect the dynamics of ligand recognition. The study was focused on *three key interactions*, namely *a*) the *ionic bond* between the ammonium head and Asp103; *b*) the *H-bond* of the ester C=O group with Asn404; and *c*) the *H-bond* of the OH group with Asn404. The docking algorithm automatically inserted the optimized ligand structure into the rigid receptor. The dynamics then began (time 0) by allowing both the binding site and the ligand to optimize their conformation and interactions.

The *upper plot* on the right-hand side shows the variation of the *distance between the ester C=O group and Asn404*. This distance remained almost constant around 2.5 Å for (*S*)-hyoscyamine (*red trace*). Also the distance for (*R*)-hyoscyamine (*blue trace*)

remained nearly constant but was larger (5.5 Å) despite a mutual protein–ligand adaptation during the simulation.

For each monitored interaction, the *Table* on the left compiles averages, minima, maxima, and ranges. The values confirm that the receptor complex with (*R*)-hyoscyamine exhibits weaker interactions characterized by a greater variability compared to (*S*)-hyoscyamine. A more careful comparison of *the average distances* reveals that the first two distances in the *Table* show minimal differences between the two simulated complexes; in contrast, the *CO*···*Asn404 distance* displays a marked difference between the two complexes and appears to play a *key role in determining the observed stereoselectivity of hmAChR2*. This confirms that, while the key salt bridge with Asp104 is a mandatory interaction for ligand affinity, the *main enantiomeric discrimination* is due to the ability of (*S*)-hyoscyamine to elicit a stable bidentate interaction with Asn404, as already seen in the docking analyses discussed above.

When considering the *minimal and maximal distance values* in the two hmAChR2 complexes, one may observe that the differences in the $N^+ \cdots$ Asp103 and OH··· Asn404 remains modest. In contrast, the CO··· Asn404 distances differ markedly not only in their mean values as discussed above, but in their minima and maxima. The higher maximal value of the (*R*)-hyoscyamine complex may also indicate a greater mobility, suggesting that the receptor can accommodate this ligand only through large and energetically expensive conformational shifts, a fact that affects negatively the stability of the complex.

A better understanding of the different mobilities of the two simulated complexes can also be gained from the *lower plot* on the right-hand side containing the *RMSD variations* computed when considering only the ligand plus the residues included in a 5-Å-radius sphere around it. One may note that the two profiles differ substantially during the entire simulation. Thus, the RMSD of the (*S*)-hyoscyamine complex (*red line*) is clearly constant with very small variations and indicates a marked stability. In contrast, the RMSD profile of the (*R*)-hyoscyamine complex (*blue line*) shows a sharp increase at the beginning of the simulation and then ample fluctuations in the range of 2–5 Å. The initial increase suggests a mutual adaptation between ligand and receptor. This adaptation appears negligible for the (*S*)-hyoscyamine complex but requires significant and energetically expensive conformational shifts to accommodate (*R*)-hyoscyamine. In the remaining part of the simulations, the larger and more fluctuating RMSD values of the (*R*)-hyoscyamine complex indicate that the receptor tries to optimize key interactions with the ligand, but this process remains substantially unproductive (as seen also in the upper plot) and involves continuous *conformational shifts* more expensive than those occurring in the (*S*)-enantiomer complex. Notably, the RMSD values computed for the two ligands (not shown) only are low and quite similar, thus indicating that the ligands remain stably in the binding pocket, and the observed differences are essentially due to backbone and side-chain mobility in the protein.

Thus, the simulations presented in this series of *Figures* suggest that the observed stereoselectivity can be rationalized in terms of *a*) differences in the *strength of the key interactions* stabilizing the complexes, as assessed by their distances; and *b*) the *conformational costs* required to stabilize the complexes. In other words, the simulations agree with experimental affinities and explain how and why (*R*)-hyoscyamine forms a weaker complex with its receptor targets and is a weaker muscarinic antagonist than its enantiomer.

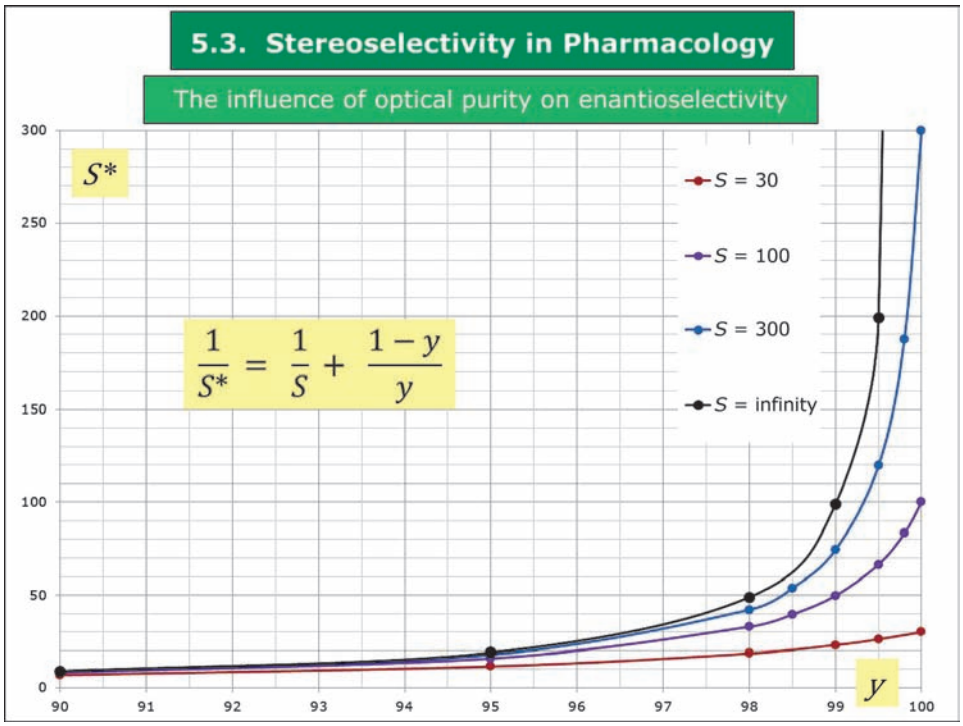

Fig. 5.16. The influence of chirality and configuration generally on pharmacological activity is discussed in a number of extensive reviews [1–8][17][61–73]. Other publications deal with specific pharmacological classes including adrenergic agents [30][74–77], psychoactive drugs [78], ion channels [79][80], and general anesthetics [81][82].

One often neglected stereochemical factor in pharmacology is the *optical purity* of the drugs or agents under study. Indeed, such analyses, like all other types of structure–activity relationships, can never be more reliable than the experimental data on which they are based. Quantitative definitions of *optical purity* (% OP), *enantiomeric purity* (% EP), *enantiomeric excess* (% ee), and *enantiomeric* % were given in *Part 1* (*Fig. 1.18*, *Eqns. 1.4–1.6*). Here, we consider the often overlooked implications of the *degree of enantiomeric purity on the relative activities of enantiomers*. Indications such as *'The optical purity was better than 98%'* are commonly found, but the limitations of the usual analytical or synthetic methods are generally ignored [83]. That the degree of enantiomeric purity markedly and even dramatically influences the apparent stereoselectivity was established beyond doubt four decades ago by *Barlow et al.* [84]. Their simulations replotted here show that the *apparent stereospecific index* S* depends strikingly on both the *enantiomeric purity* y and the *true stereospecific index* S, a dependence which increases exponentially as *y* and *S* increase. This should be a cause of worry for many workers, but the warning has been all but ignored despite experimental proofs of its validity ([84] and next *Figure*).

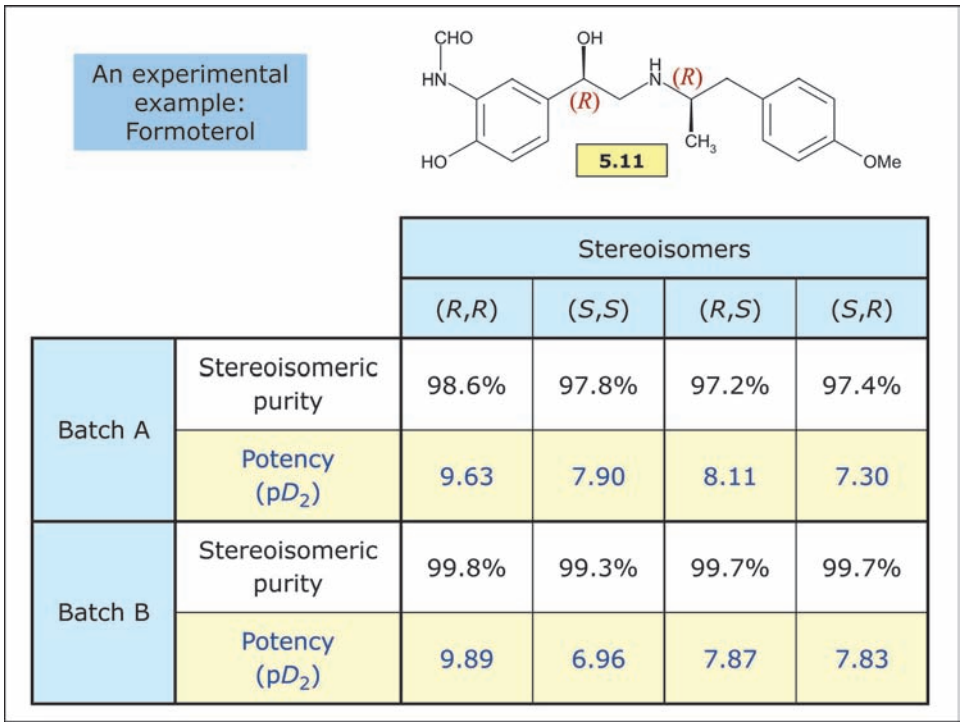

		Stereoisomers			
		(*R*,*R*)	(*S*,*S*)	(*R*,*S*)	(*S*,*R*)
Batch A	Stereoisomeric purity	98.6%	97.8%	97.2%	97.4%
	Potency (pD_2)	9.63	7.90	8.11	7.30
Batch B	Stereoisomeric purity	99.8%	99.3%	99.7%	99.7%
	Potency (pD_2)	9.89	6.96	7.87	7.83

Fig. 5.17. Strong experimental evidence has since confirmed that marked differences in potency ratios exist between stereoisomers having good (*ca.* 98%) or excellent (*ca.* 99.7%) degrees of purity. *Formoterol* is a β_2-adrenoceptor agonist with two stereogenic centers, allowing the possibility of gaining more information than with a pair of enantiomers. The most active stereoisomer is the (*R*,*R*)-form **5.11** [85][86]. Looking first at *Batch A*, we find that the stereoisomeric purity of the four stereoisomers ranges from 97.2% to 98.6%, values generally recognized as good levels of purity in such studies. The pharmacological response examined was the *potency* (*i.e.*, the concentration of a drug necessary to obtain 50% of the maximal response); note that potencies are reported as negative logarithms ($-\log D_2$, written as pD_2) such that higher values indicate higher potency. The activity ranking in this batch is $(R,R) \gg (R,S) \approx (S,S) > (S,R)$, while the differences in activity are two orders of magnitude for the $(R,R)+(S,S)$ pair, and one order for the $(R,S)+(S,R)$ pair.

Batch B has a different story to tell, and its comparison with *Batch A* is particularly revealing. Extensive purification gave individual enantiomers with purities of 99.3% to 99.8%. The altered activity ranking now becomes $(R,R) \gg (R,S) \equiv (S,R) > (S,S)$. Furthermore, the differences in activity are now *three* orders of magnitude for the $(R,R)+(S,S)$ pair, while the (*R*,*S*)- and (*S*,*R*)-enantiomers are found to be equiactive, in marked contrast to the result for *Batch A*.

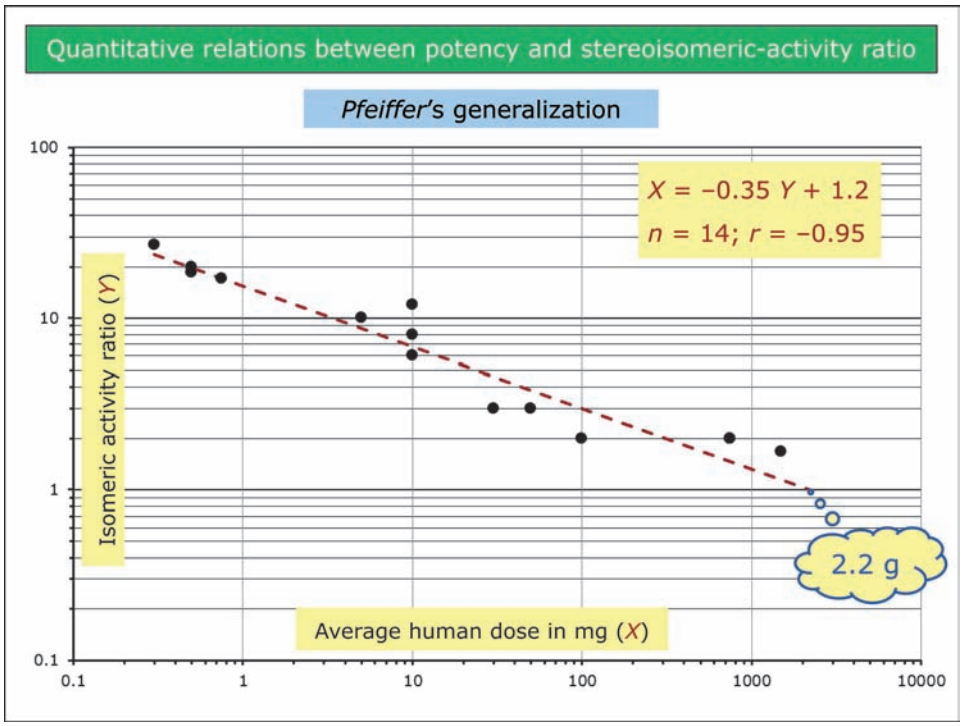

Fig. 5.18. A landmark generalization relating pharmacological activity and chirality was attained by *Pfeiffer* [87]. He showed that some pharmacological data can be rationalized such that *the more active the racemate, the larger the enantiomeric activity ratio*. Indeed, *Pfeiffer* found a linear relationshisp between the logarithm of the activity ratio of enantiomers (Y) and the logarithm of the average human dose of the racemate (X), the slope being -0.35, the intercept 1.2, and the correlation coefficient -0.95. The data points and regression line have been redrawn here from the compiled data. An interesting feature of the regression line is that it intercepts with unity (equal activity of the enantiomers) at a dose of 2.2 g.

While the term '*Pfeiffer*'s rule' is generally used in the literature, the original author was careful to refer to a '*generalization*'. Yet despite its rightful impact, this study suffers from various limitations, especially *a*) the highly hybrid nature of the *in vivo* activity parameter used, which depends on many pharmacokinetic factors besides intrinsic activity, and *b*) the degree of optical purity, which, as we saw, can have a marked influence on the enantiomeric-activity ratio. And indeed, numerous exceptions to this generalization have been found [88]. Another significant observation made years ago is that the influence of configuration can be large or small depending whether the stereogenic center is located in a critical or non-critical part of the drug, namely in a moiety playing an essential or accessory role in receptor binding [89].

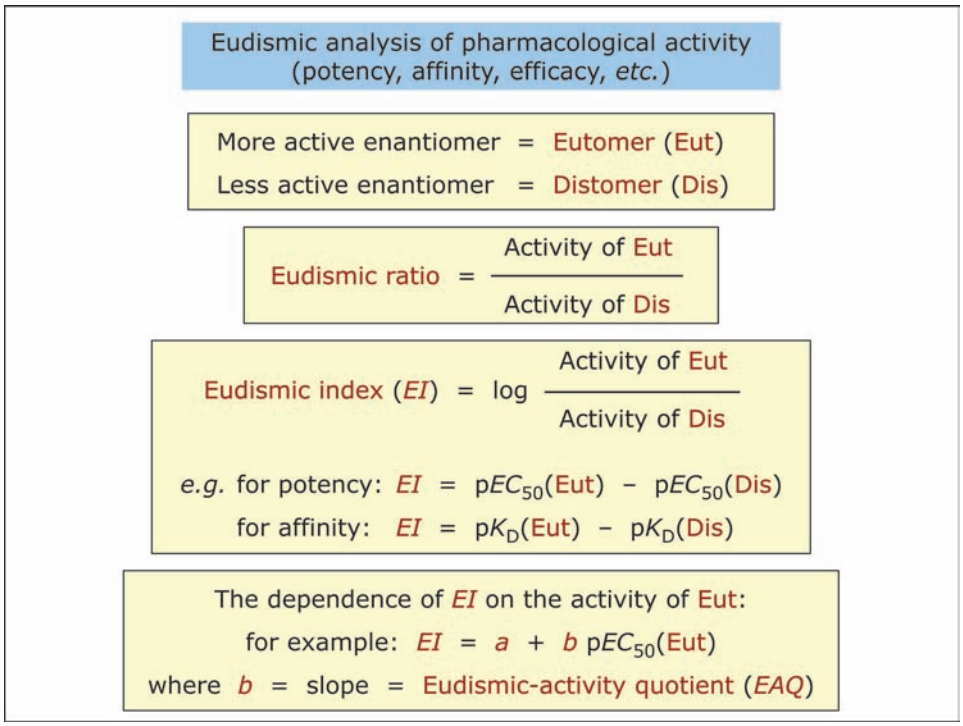

Fig. 5.19. *Pfeiffer*'s generalization has inspired other workers to search for similar relationships and to express them in a more formal way. Thus, *Lehmann* developed what he termed '*eudismic analysis*', a quantitative approach to relate the activity of the more potent enantiomer to the stereoisomeric-activity ratio [90–92]. He began by proposing the useful and widely used terms '*eutomer*' and '*distomer*' to designate the more and lesser active enantiomer, respectively. The meaning of '*activity*' as used here should be taken to cover any of its components such as *affinity*, *potency*, and *efficacy*. In fact, most eudismic analyses deal with data of affinity to pharmacological targets, but the approach has been extended to both substrates and inhibitors of drug-metabolizing enzymes. Furthermore, the terms 'eutomer' and 'distomer' are not restricted to enantiomers but may also be applied to pairs of diastereoisomers.

The next definition is that of the '*eudismic ratio*' (the ratio of activities), a useful term conveniently replacing the clumsy expression we have used up to now, namely the 'enantiomeric activity ratio'. The logarithm of the eudismic ratio is called the '*eudismic index*' (*EI*), again a particularly useful term, since many parameters of activity are expressed in negative log form (see *Fig. 5.17*).

Eudismic analysis has proven particularly informative when studying series of congeneric pairs of enantiomers. This has been accomplished by plotting the activity of the eutomer against the eudismic index. When a linear correlation was obtained, its slope was called the '*eudismic-activity quotient*'.

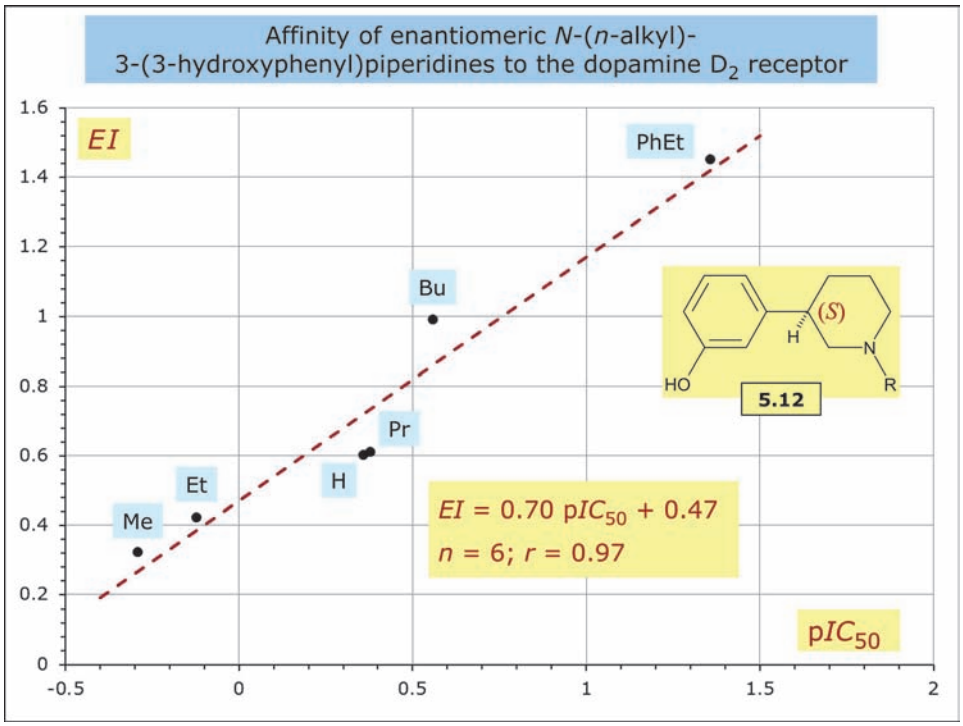

Fig. 5.20. Eudismic analysis is illustrated here with a series of six enantiomeric pairs of N-(n-*alkyl)-3-(3-hydroxyphenyl)piperidines* (**5.12**) [93]. Their binding to the *dopamine D_2 receptor* was determined by displacement of the labeled ligand [^{3}H]spiperone, yielding the affinity constant IC_{50}. The correlation coefficient between affinity and eudismic index was a good one, and the slope indicated a marked contribution of the stereogenic center to activity.

Perhaps the greatest benefits of eudismic analysis have been obtained when comparing the slopes for one chemical series of ligands binding to different receptors, or for several chemical series binding to a given receptor [92][94]. However, one should not conclude from the above that eudismic analysis is consistently successful. In most published examples of eudismic analysis, plotting the activity of the eutomer against the eudismic index indeed led to a statistically fair or good linear correlation – but the absence of correlation is seldom if ever treated as a publishable result! A case in point is a detailed study of seven enantiomeric pairs of congeneric hexahydropyrazinoquinolines with high affinity and selectivity toward the dopamine D_3 receptor [95]. Not only was there no correlation between affinity and eudismic index, but the absolute configuration of the eutomer was (*S*) in three cases and (*R*) in the four other cases. This suggests variable modes of binding, a valuable piece of information in itself.

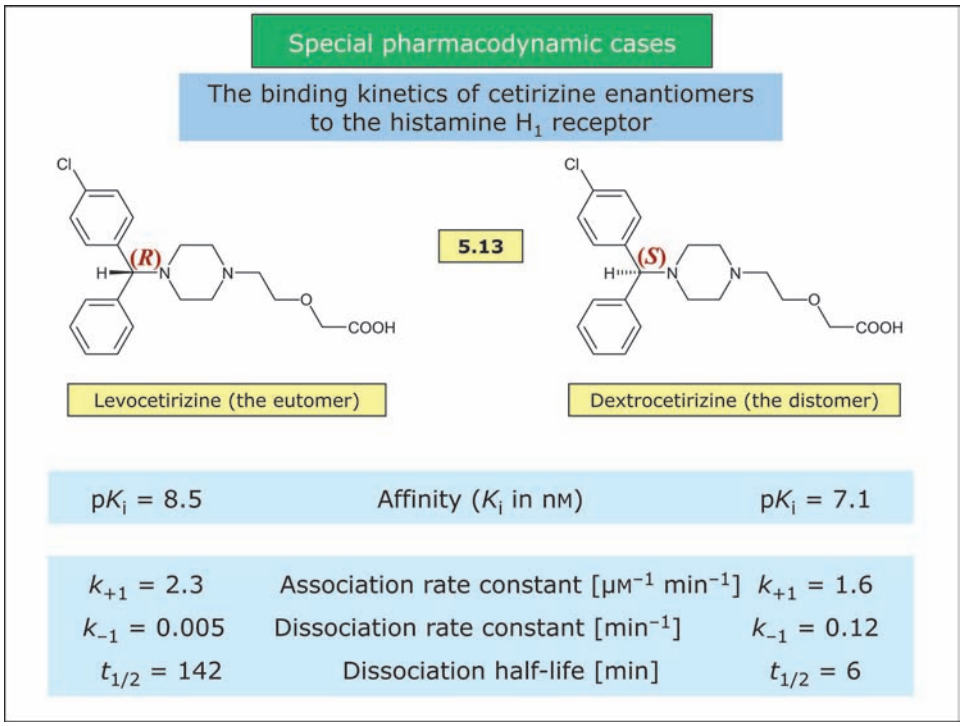

Fig. 5.21. In this and the next *Figures*, we turn our attention to a few special cases of stereoselectivity encountered in pharmacological studies. The first example is that of *cetirizine* (**5.13**), a potent non-sedating anti-allergic drug which acts by antagonizing histamine H_1 receptors [96]. When enantioselectivity was assessed by the *equilibrium dissociation constant* K_i, a modest eudismic index ($\Delta(pK_i) = 1.4$) was found to separate the two enantiomers, suggesting levocetirizine to be more potent than dextrocetirizine by only one order of magnitude. This is in contrast with clinical activity data which show that the activity of racemic cetirizine is almost entirely accounted for by its *eutomer levocetirizine*. This discrepancy strongly suggests that the equilibrium dissociation constant of cetirizine enantiomers offers an incomplete description of their interaction with the histamine H_1 receptor. This was verified when the individual *rate constants of association and dissociation* were determined, showing that, while the rate constant of formation of the receptor–ligand complex (k_{+1}) was comparable for both enantiomers, the dissociation of levocetirizine from the receptor complex (k_{-1}) was *ca.* 25 times slower than that of dextrocetirizine. In other words, the much greater activity of levocetirizine is principally due the prologued stability of the complex it forms with the H_1 receptor. Stated differently, levocetirizine acts as a pseudo-irreversible receptor antagonist in functional studies [97].

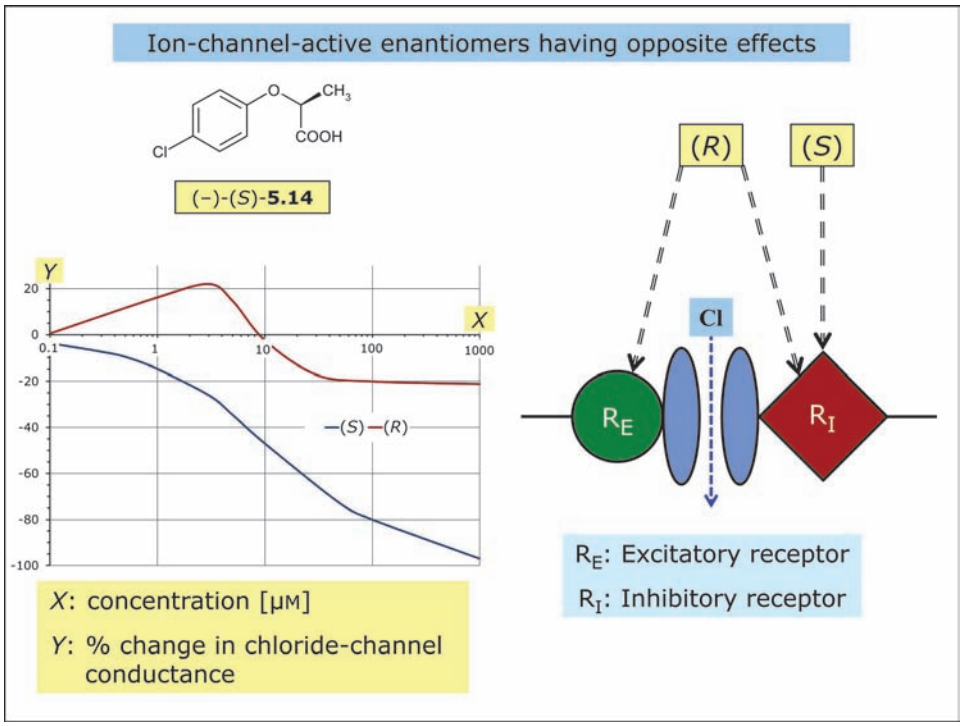

Fig. 5.22. A number of drug classes act at *ion channels* either to *block or activate* them. The best known example is perhaps that of *dihydropyridines*, a medicinal class in which antagonists block transmembrane Ca^{2+} influx, thereby causing relaxation of smooth and cardiac muscles. Interestingly, there are examples of *enantiomers showing opposite effects* at ion channels, raising the problem of their molecular mechanism of action [66][67][79][80]. Part of the answer came when it was shown that the enantiomers of an experimental dihydropyridine acted at different sites on the voltage-dependent calcium channel of vascular muscle [98].

Using *phenoxypropionic acid analogs* as model compounds, it was demonstrated that their enantiomers had opposite actions on rat skeletal muscle chloride channels [99]. The model compound *2-(4-chlorophenoxy)propionic acid* (**5.14**) proved particularly intriguing (left pannel in the *Figure*). Its (*S*)-enantiomer behaved as a *full antagonist*, whereas the (*R*)-enantiomer was an *apparently weak activator* at low concentration and a *weak antagonist* in the high concentration range. This behavior was modeled quantitatively by assuming a molecular machine consisting in *two regulatory sites* controling the chloride channel, namely an excitatory and an inhibitory one (right pannel) [100]. In this model, the (*S*)-enantiomer acted only on the inhibitory site. In contrast, the (*R*)-enantiomer acted on both sites, excitation peaking at 3 μM and inhibition dominating progressively above this concentration.

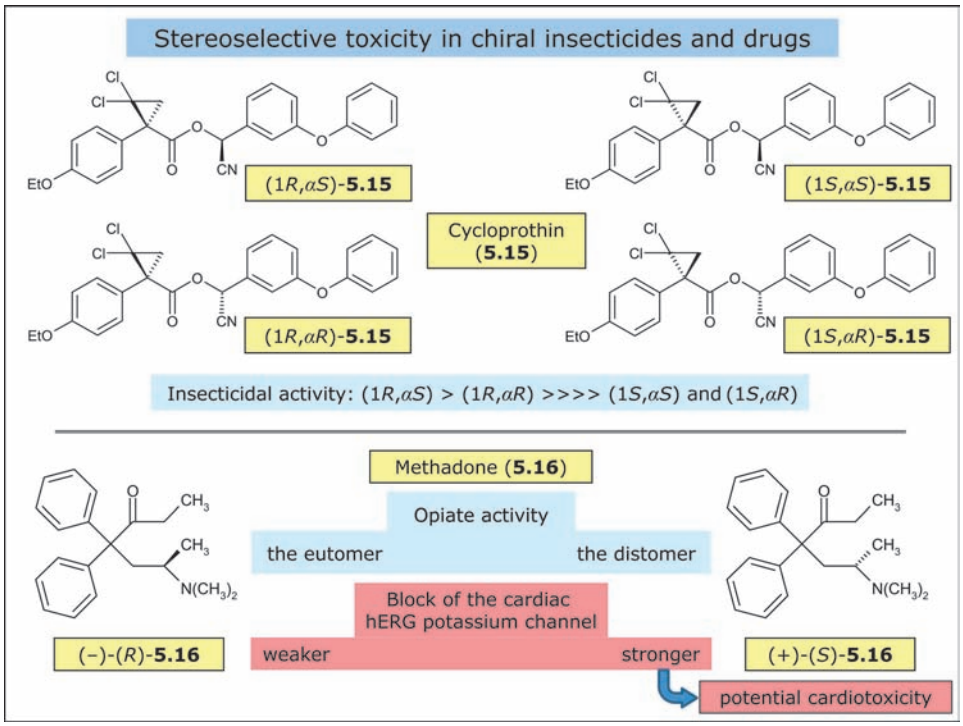

Fig. 5.23. *Toxicity* is a major *cause of concern* in drug research, but also a *target activity* in some agrochemicals designed to control pests such as insects. Whether wanted or unwanted, toxicity is also a biological response subject to stereoselectivity. Here, we use cycloprothin to exemplify stereoselective toxicity in insecticides [7], and methadone as an apt illustration of an enantioselective adverse drug reaction.

Cycloprothin (**5.15**) contains two stereogenic centers, one labeled C(1) by the authors of the study, and the other C(α) [101]. The four stereoisomers were screened for insecticidal activity against larvae of two insect species. As shown, configuration at C(1) proved critical for activity, whereas the effect of that at C(α) was marginal.

Fig. 5.22 has presented enantiomers acting differently on two regulatory sites, a situation we can extend to *unrelated pharmacological sites*. This is seen when one enantiomer produces the clinically beneficial effects, while the other accounts for adverse reactions, as illustrated by *methadone* (**5.16**). Methadone is a well-known agonist of the μ-opiate receptor and is used as the racemate, although its (*R*)-enantiomer is the *eutomer* accounting for this wanted activity. Recent studies have demonstrated that methadone inhibits the *human cardiac hERG potassium channel* [102]. This worrying mechanism of *cardiotoxicity*, which has resulted in the withdrawal of several marketed drugs, can be monitored in electrocardiograms as *prolongation of the QT interval* [103][104]. While both enantiomers of methadone inhibit the hERG channel, a clear enantioselectivity was demonstrated with (*S*)-methadone proving 3–4 times more active than the analgesic eutomer. A small clinical study has confirmed the beneficial effect of replacing racemic methadone with the (*R*)-enantiomer in maintenance patients [105].

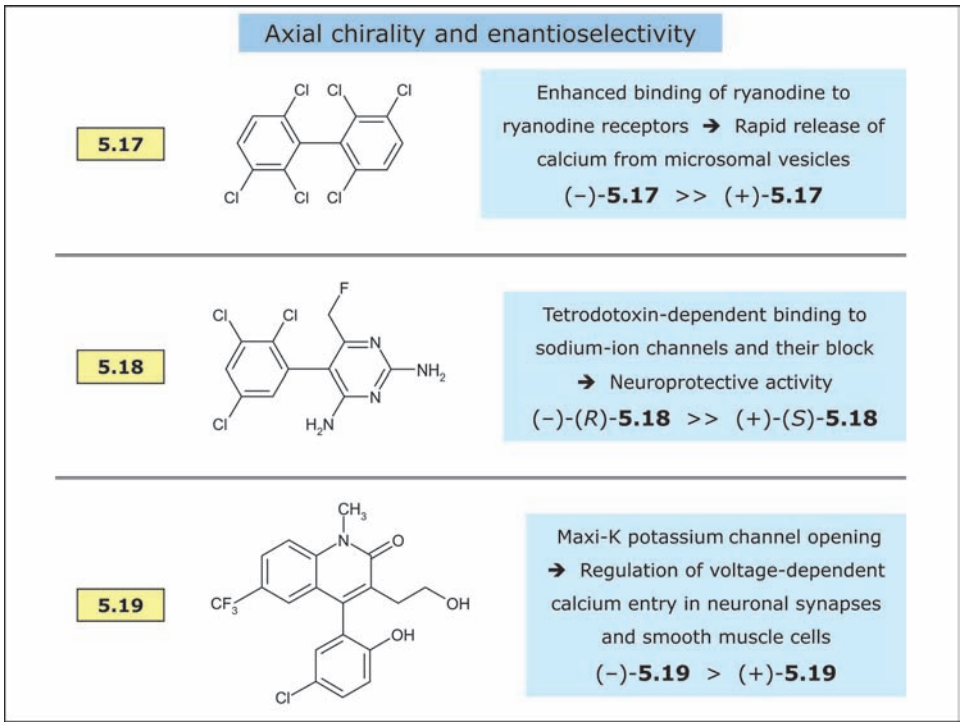

Fig. 5.24. So far, our examples have dealt with central chirality – but what about *axial chirality*? Here, we present three pairs of enantiomeric atropisomers to illustrate their enantioselective activity at *ion channels*. Note that all three pairs are configurationally stable under pharmacological conditions. Our first example is *2,2′,3,3′,6,6′-hexachlorobiphenyl* (**5.17**; also known as PCB 136), a well-known POP (*persistent organic pollutant*). Its (−)-enantiomer was found to enhance the binding of ryanodine to its receptors, most likely by binding to a regulatory site, thereby inducing a rapid release of calcium ions from microsomal vesicles [106]. The (+)-enantiomer was devoid of effect. This finding throws a new light on the toxic potential of PCB 136.

Our other examples are drug candidates, namely *BW202W92* (**5.18**) [107] and *4-(5-chloro-2-hydroxyphenyl)-3-(2-hydroxyethyl)-1-methyl-6-(trifluoromethyl)quinolin-2(1*H*)-one* (**5.19**) [108]. The former is a potent and selective sodium-ion-channel blocker and a potent neuroprotective agent in *in vivo* models of cerebral ischemia and stroke damage. The two enantiomers of BW202W92 (**5.18**) were separated, their absolute configuration determined, and the (*S*)-enantiomer was found to be much less active than the (*R*)-form. A comparable situation is encountered in case of compound **5.19**, where the (−)-atropisomer was the eutomer in opening maxi-K channels.

Taken together, these three examples demonstrate that axially chiral agents may show enantioselectivity just like centrally chiral ones. But just like the latter (see *Part 2*), in vivo *racemization* may be a confounding factor [109], although it did not play a role in these three examples.

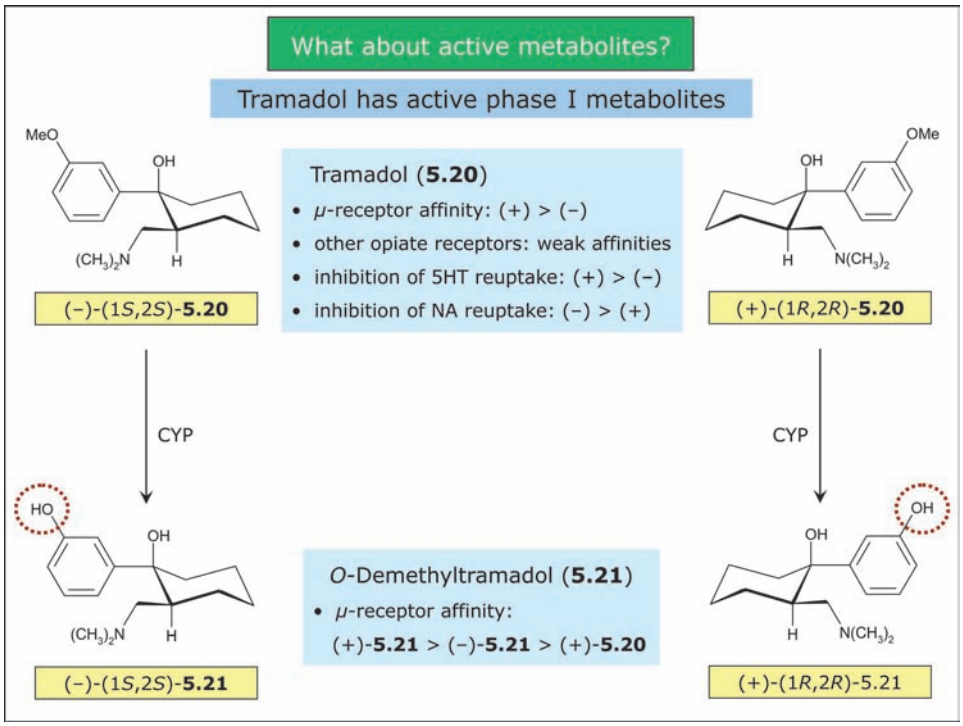

Fig. 5.25. An additional dimension to be considered when investigating stereoselectivity in pharmacodynamic processes is the contribution of active metabolites [110]. This significant aspect is illustrated here and in the next *Figure*.

Tramadol (**5.20**) is a frequently used centrally acting analgesic which combines a high efficacy, a low potential for abuse or dependence, and a low level of side-effects, notably the absence of respiratory depression or effects on blood pressure and heart rate [111–115]. This drug is particularly noteworthy for its dual mechanism of action, being both a weak *opioid agonist* and an *inhibitor of monoamine neurotransmitter reuptake*. For good reasons, the drug is used as the *racemic mixture of two of its four stereoisomers*, *i.e.*, the (+)-(*R*,*R*)- and (−)-(*S*,*S*)-form, as these two enantiomers contribute in a complementary manner to its *in vivo* activity. Indeed, in *experimental pharmacology* (+)-(*R*,*R*)-tramadol proved a more active *μ-receptor agonist* than its (−)-(*S*,*S*)-enantiomer, and it also inhibited serotonin reuptake. In contrast, the (−)-(*S*,*S*)-enantiomer is the better inhibitor of noradrenaline reuptake in addition to its weaker opioid effects. Furthermore, both enantiomers are metabolized by cytochrome P450 (CYP) to the corresponding O-*demethyltramadol enantiomers*, **5.21**, with little or no substrate enantioselectivity. Both enantiomers of *O*-demethyltramadol are *more active* than (+)-(*R*,*R*)-tramadol as *μ*-receptor agonists, but their blood–brain-barrier permeation is somewhat lower. The effects of these metabolites on monoamine neurotransmitter reuptake have not been reported. In *clinical pharmacology*, tramadol-induced analgesia is thus found to result from the *combined effects of four active entities*, namely (*R*,*R*)- and (*S*,*S*)-tramadol plus their *O*-demethyl metabolites.

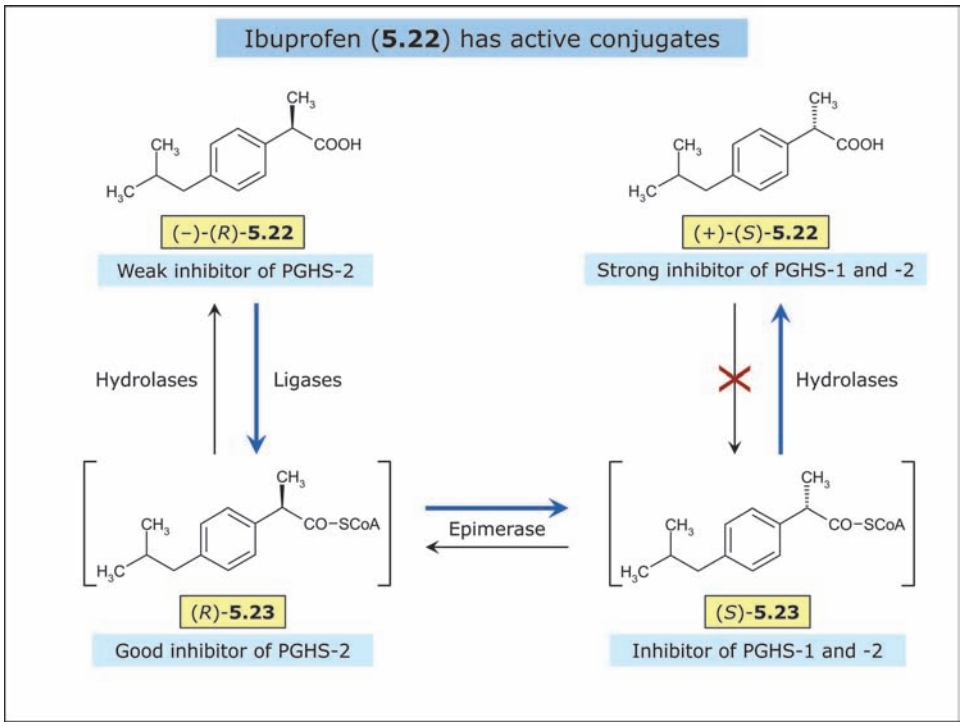

Fig. 5.26. *Ibuprofen* (**5.22**) is a non-steroidal anti-inflammatory 2-arylpropanoic acid (*i.e.*, a profen) extensively used as the racemate (see also *Part 8*) [116–119]. The clinical activity of the drug is due mainly to its inhibition of *prostaglandin-H synthases* (PGHS), an activity that resides in the (*S*)-enantiomer. The (*R*)-enantiomer, while contributing little to activity as such, undergoes an intriguing metabolic reaction that has attracted much interest, namely *its inversion of configuration to the eutomer*. The first step in this activation pathway (*blue arrows*) is the formation of an *acyl-Coenzyme A conjugate*, **5.23**, a reaction catalyzed mainly by *long-chain acyl-CoA ligase* [120][121]. This reaction is *enantioselective* in that it shows a marked or practically exclusive preference for (*R*)-profens. In other words and in the case of ibuprofen, the ligase forms practically only the *(*R*)-ibuprofenoyl-CoA*. Once formed, this conjugate is the substrate of a reaction of *epimerization* (CoA being itself chiral) catalyzed by *2-methylacyl-CoA 2-epimerase*, a peroxisomal and mitochondrial enzyme catalyzing an essential step in the oxidation of cholesterol to cholic acid [121][122]. As a result of epimerization, the ibuprofenoyl moiety now exists in the (*R*)- and (*S*)-forms, and *acyl-CoA thioesterases* act on both (*R*)- and (*S*)-ibuprofenoyl-CoA to liberate the corresponding ibuprofen enantiomer. In the metabolic scheme shown here, (*S*)-ibuprofen is thus an end point only, not an entry point; in contrast, (*R*)-ibuprofen is both. A further point of interest in our discussion is the fact that (*R*)-ibuprofenoyl-CoA, and (*S*)-ibuprofenoyl-CoA to a lesser extent, were found to be *inhibitors of PGHSs* and thus may contribute to the clinical response [123][124].

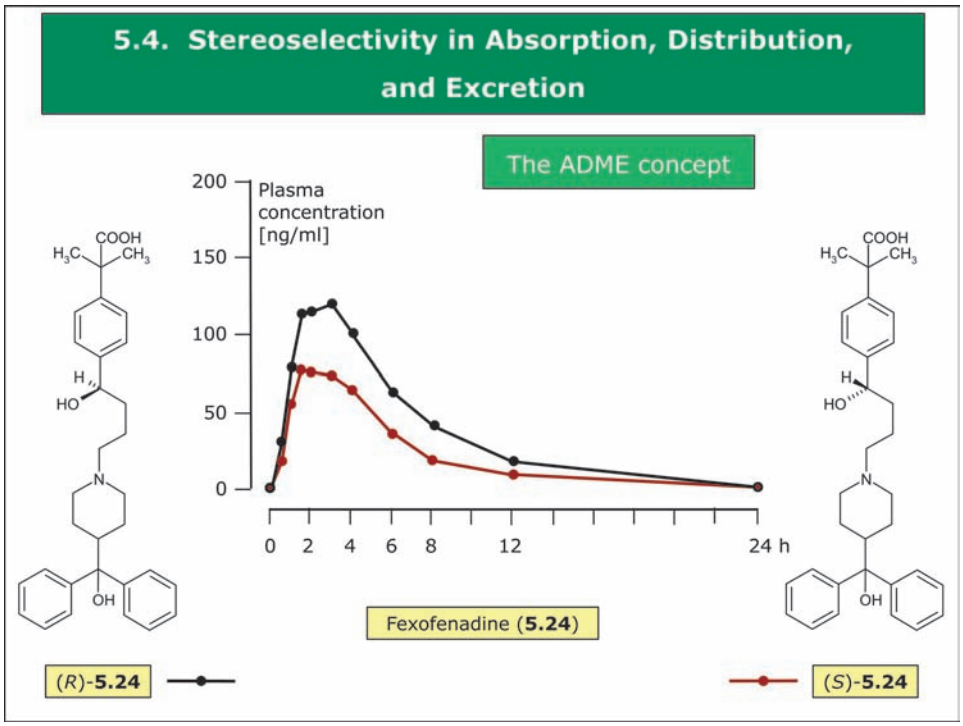

Fig. 5.27. *Part 5* concludes with a *Chapter* on stereochemically relevant aspects of *Absorption, Distribution, and Excretion*. These pharmacokinetic processes are part of the well-known and global concept of *ADME* [125–127] which also includes *Metabolism* to which *Parts 7* and *8* are dedicated. The literature offers numerous examples of *stereoselective pharmacokinetics* in humans and animals (*e.g.*, [115][128–135], but the biological factors which account for the differences observed between stereoisomers, when such differences are confirmed and statistically significant, are not easy to disentangle. Indeed, a mechanistic interpretation, especially when multifactorial, is difficult to conceive and calls for lengthy *in vivo* and *in vitro* investigations.

To take but a single example, we look here at the behavior of *fexofenadine* (**5.24**), a histamine H_1-receptor antagonist drug used extensively to alleviate allergic symptoms. This chiral drug is used as the racemate, with both enantiomers being equipotent. In healthy subjects administered an oral dose of the racemic drug, a 24-h monitoring of their plasma concentrations showed marked differences between the two enantiomers [136]. Thus, the *areas-under-the-curves* (AUCs) were 850 ± 150 and 500 ± 130 (ng h)/ml for the (*R*)- and (*S*)-enantiomer, respectively, while their elimination half-lives were comparable. Knowing that fexofenadine is poorly metabolized (at most a few %) and *extensively excreted unchanged* in urine and feces, a role for the transporter *P-glycoprotein* (P-gp) was postulated. However, this remained a weak hypothesis until extensive investigations showed that a number of transporters are involved in the *weakly enantioselective distribution and transport* of fexofenadine [137].

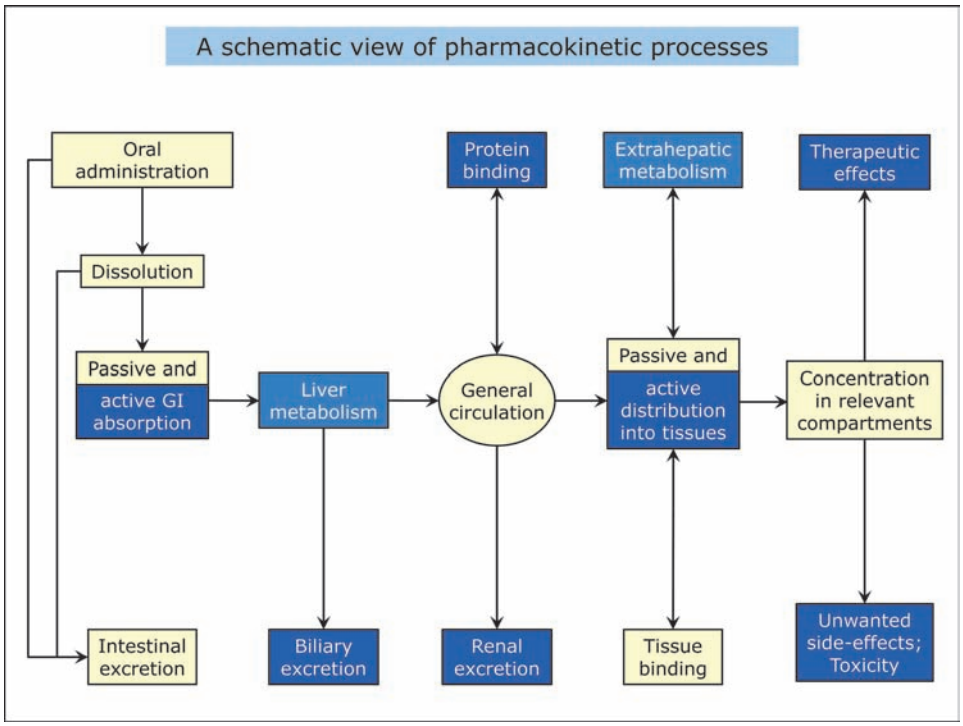

Figs. 5.28 and 5.29. A brief introduction to the ADME concept is offered below, while the two *Figures* present a schematic view of the concept as illustrated in the present section. This is done to identify the main *biochemical mechanisms* involved in drug disposition throughout the body in order to discern the possible impact of stereochemistry upon these mechanisms.

The first process is *absorption*. Drugs and other non-nutrient xenobiotics may gain access to the body by a remarkable number of routes. By far the most important of these are those used by the body for its own metabolism, namely the *gastrointestinal (GI) tract* and the *airways*, including the lungs where gas exchange occurs. In addition, numerous compounds enter *via* the *skin*, which behaves as an active organ rather than an inert barrier separating the *milieu intérieur* from the outside world. On occasion, compounds may enter *via* one of the various orifices of the body. As far as drugs are concerned, numerous artificial means of entry are employed, generally divided into *enteral* (gastrointestinal tract and the like), *parenteral* (the various routes of injection), and *topical* (through skin and mucosae) routes.

In each of these portals of entry, a compound must pass through a series of membranes, entering and then leaving the circulating blood, to reach the target site at which it exerts its action. At this stage, absorption has changed to *distribution*. These same *membrane barriers* which limit absorption also govern the access of the compound to the enzymes catalyzing its *metabolism* (*i.e.*, chemical elimination). Ultimately, membrane barriers also govern the *excretion* (*i.e.*, physical elimination) of a compound and its metabolites through one or other of the *excretory pathways*. The principal routes of excretion are *via* the *kidney* into the urine, or *via* the *liver and bile*

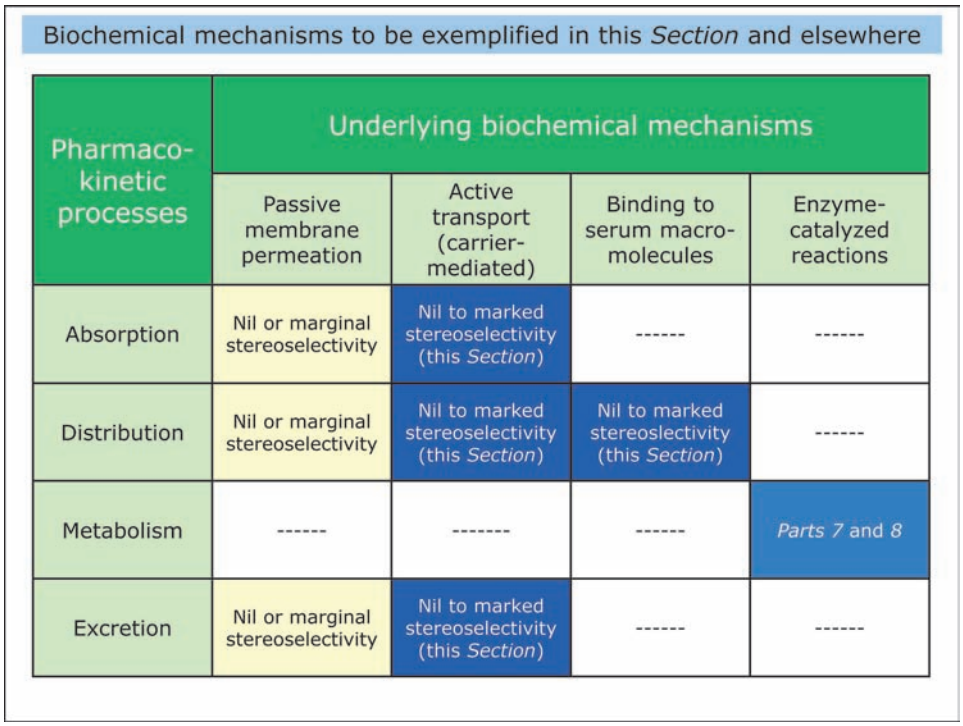

Fig. 5.29.

ultimately leading to loss in the feces. In addition, several other pathways, quantitatively less important, may contribute to excretion, but these are not relevant here.

The most frequent way by which drugs cross cell membranes is *passive membrane permeation* and more generally *passive diffusion* down a concentration gradient, from high to low [138–141]. The great majority of drugs are either weak acids or bases, which thus exist in ionized and unionized forms depending on the pH. Characteristically, the unionized forms are more lipophilic and thus diffuse readily across lipid-rich membranes. The rate and extent of membrane passage is thus a function of the *ionization*, readily expressed by pK_a, and *lipophilicity*, denoted by log *P*, of the drug in question. Note that protonation decreases the lipophilicity of amines by roughly three log *P* units, while deprotonation decreases the log *P* of carboxylic acids by roughly four units [142]. But since *enantiomers* are not differentiated at all in terms of these physicochemical properties, and *diastereoisomers* only modestly so [143], passive diffusion is at best only marginally influenced by drug stereochemistry and will not be considered in our context.

The remainder of this section is devoted to two stereoselective processes which contribute to drug absorption, distribution, and excretion, namely active (energy-consuming) transport by *membrane carrier proteins* and *binding to and transport by serum macromolecules.*

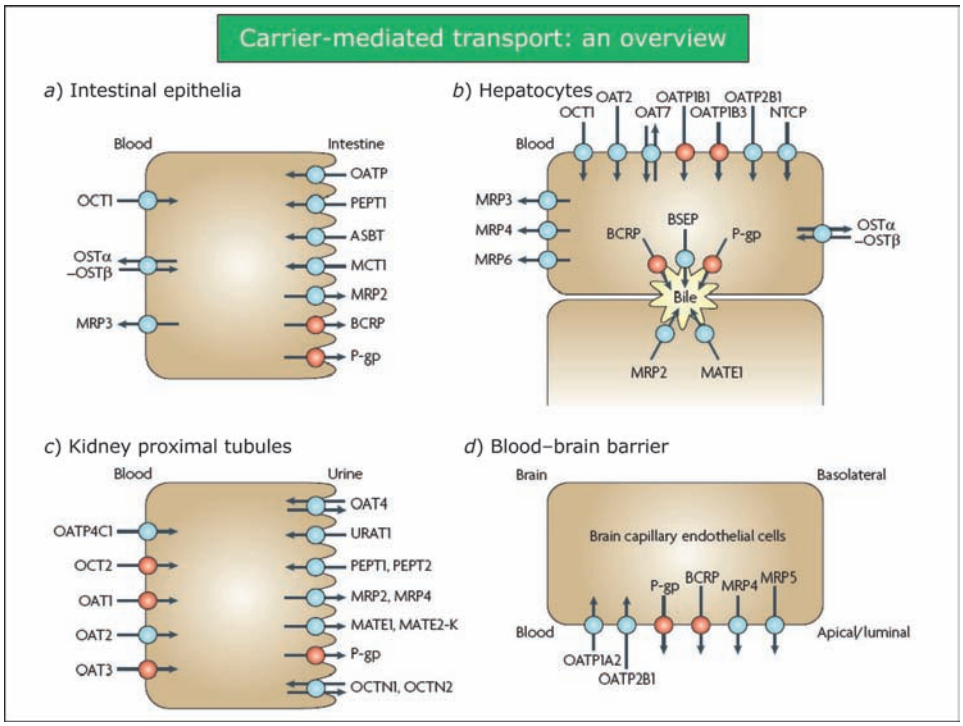

Fig. 5.30. *Membrane transport proteins* (also known as transporters or carriers) govern the transport of xenobiotics and endogenous compounds in and out of cells. They have critical roles in the pharmacokinetic behavior of many drugs, with potential impact upon safety and efficacy [144 – 146]. The transporters are found throughout the body, their most important tissue locations being illustrated in the *Figure* (reproduced from [147] with permission), where arrows pointing out of cells indicate *efflux pumps*, whereas arrow pointing into cells represent *transport into cells*. Their locations are primarily in organs and tissues associated with the entry and exit of drugs into and out of the body.

There are more than 400 currently known unique human transporters, and the body of evidence is growing rapidly for their roles in drug absorption, distribution, and excretion, as well as drug–drug interactions. Of these more than 400, *seven are currently recognized as particularly important* and are *indicated in red* in the *Figure*. They are the permeability glycoprotein (*P-glycoprotein* (P-gp), MDR1, ABCB1), the *breast cancer resistance protein* (BCRP, ABCG2), the *organic acid transporter 1* (OAT1 (SLC22A6)), *OAT3* (SLC22A8), the *organic anion transporting polypeptide* (OATP1B1 (SLCO1B1)), *OATP1B3* (SLCO1B3) and the *organic cation transporter 2* (OCT2 (SLC22A2)). Other transporters include the apical sodium/bile acid co-transporter (ASBT), the bile salt excretion protein (BSEP), the multidrug and toxin extrusion protein (MATE), the sodium/taurocholate co-transporting peptide (NCTP), the organic solute transporter (OST), the peptide transporter (PEPT), and the urate transporter (URAT).

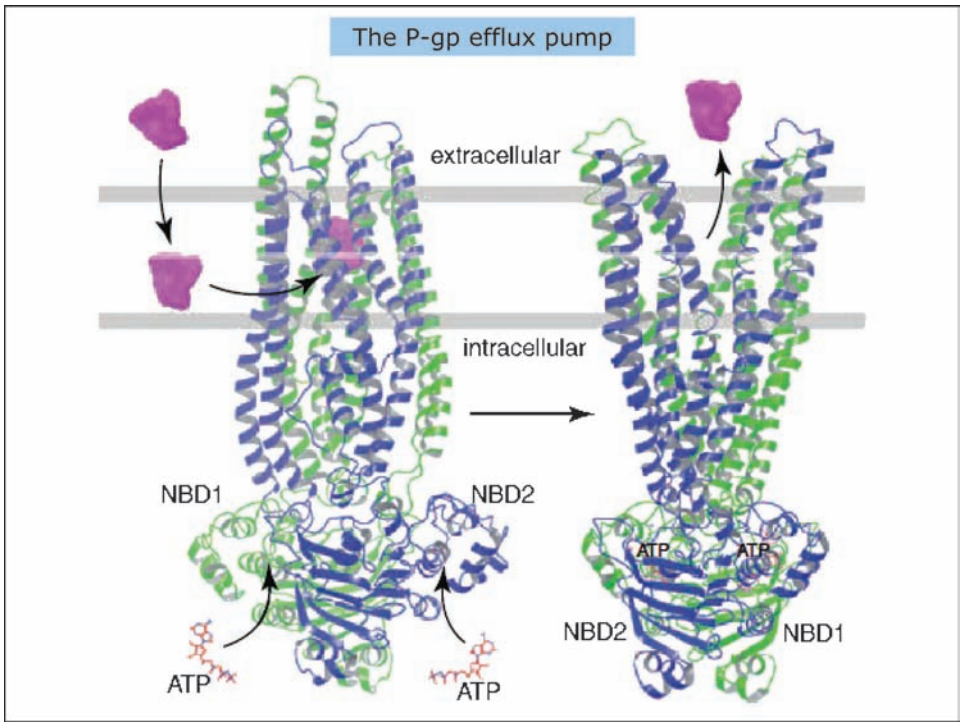

Fig. 5.31. These transporters are all energy-requiring active membrane pumps which function by the reversible binding of the drug to one or more subunits in the pump's structure. Like other drug targets, these proteins exist in a defined three-dimensional form, and binding to them has the potential to discriminate between stereoisomeric drugs, a point we shall illustrate below.

The *crystal structure of P-gp* has recently been reported [148]; as shown here, this efflux pump functions by capturing a compound (here in red) as it attempts to cross the cellular membrane and expells it back into the extracellular medium (reproduced from [149] with permission). The protein features ATP-binding domains in its intracellular segments, and a large and hydrophobic binding cavity in its transmembrane part. Molecular modeling and docking methods have been applied to examine P-gp binding specificity using binders and nonbinders [150][151]. It appears that the *ligand selectivity* of P-gp is better understood in terms of complementary physicochemical properties of ligands and binding site, rather than being defined by specific sub-sites.

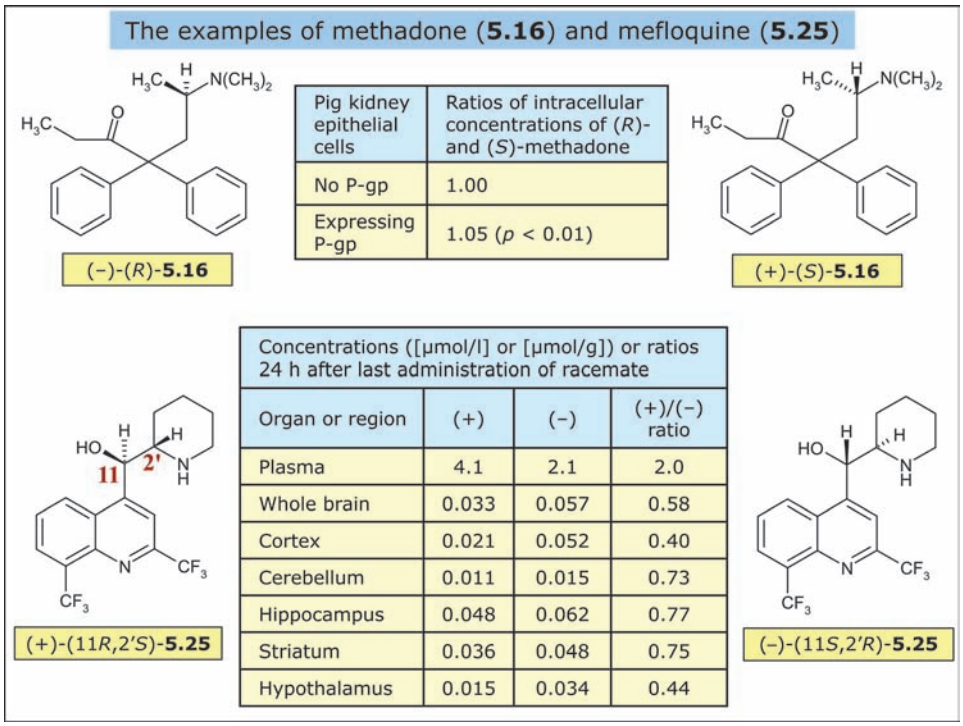

Pig kidney epithelial cells	Ratios of intracellular concentrations of (*R*)- and (*S*)-methadone
No P-gp	1.00
Expressing P-gp	1.05 ($p < 0.01$)

Concentrations ([µmol/l] or [µmol/g]) or ratios 24 h after last administration of racemate

Organ or region	(+)	(−)	(+)/(−) ratio
Plasma	4.1	2.1	2.0
Whole brain	0.033	0.057	0.58
Cortex	0.021	0.052	0.40
Cerebellum	0.011	0.015	0.73
Hippocampus	0.048	0.062	0.77
Striatum	0.036	0.048	0.75
Hypothalamus	0.015	0.034	0.44

Fig. 5.32. To return to our main focus, what is there to say about *substrate stereoselectivity* in active transport [152]?

A *variety of model systems* are being used to demonstrate the roles of membrane transporters in the absorption, distribution, and excretion of numerous drugs and foreign compounds. These include cell systems expressing or engineered to over-express transporters, genetic knockout mice in which transporters are missing, and the use of drugs and other chemicals known to inhibit transporters in interaction studies. A plethora of data has been accumulated from these systems over the last decade, although there is little comparability of data due to variability between the model systems used. A valuable review by *Choong et al.* [153] compiles much of this evidence which fails to show any substantial or systematic difference between the membrane transport of pairs of enantiomers of chiral drugs from various pharmacological classes. For example, the enantiomers of highly enantioselective calcium-channel antagonists *verapamil and nifedipine* have very similar P-gp inhibitory action in cell lines, and, in accordance with this, the tissue distribution of the enantiomers of verapamil was the same in P-gp knockout and wild-type mice.

Leach et al. [154] have analyzed data on the permeability and efflux of up to 100 pairs of enantiomers from the *AstraZeneca* database on two cell lines which show no discernible difference between the permeability or efflux of enantiomers. It may seem surprising that no differences are seen in processes which are at their heart active and enzyme-driven. It appears from this analysis that the permeability and efflux processes, while active mechanisms, are often *dominated by physicochemical factors such as*

lipophilicity and ionization, determining the passive passage of compounds into and out of cell membranes.

Three examples follow to illustrate some of the outcomes of experimental investigations, be they *in vivo* or *in vitro*. The synthetic opioid *methadone* (**5.16**) is a well-known drug used in the treatment of opiate addiction. It is used as the racemate although its (*R*)-enantiomer is by far the more active one. Methadone is a known substrate of P-gp, and it was of clear pharmacodynamic interest to check whether *methadone enantiomers interacted differently with this efflux pump*. The results reported here were obtained with pig kidney epithelial cells transfected with the human *ABCB1* gene (which codes for P-gp) [155]. As shown in the upper part of the *Figure*, both enantiomers reached identical concentrations in the control cells. In cells engineered to express P-gp, however, there was a slight excess of (*R*)-methadone, indicating a marginal preference of the efflux pump for the (*S*)-enantiomer.

A clearer case of enantioselectivity, although one that does not offer a conclusive mechanistic interpretation, is provided by a study of the brain penetration of the antimalarial *mefloquine* (**5.25**), a chiral drug whose enantiomers are equiactive [156]. Rats were administered an oral dose of racemic mefloquine during a period of 22 days, and the results reported herein were obtained 24 h after the last dose. As seen in the lower part of the *Figure*, the *plasma concentration* of the (+)-enantiomer was twice that of the (−)-isomer. In contrast, the *brain concentrations* of the (−)-enantiomer were on average 1.7-fold higher than those of the other isomer, indicating an obvious enantioselectivity. This phenomenon might be due to a facilitated (active) penetration of the (−)-enantiomer. But considering the very low brain concentrations achieved (about 70 times lower than the plasma concentrations), a more likely explanation can be found in the involvement of an *efflux pump at the blood–brain barrier acting stereoselectively on the (+)-enantiomer*.

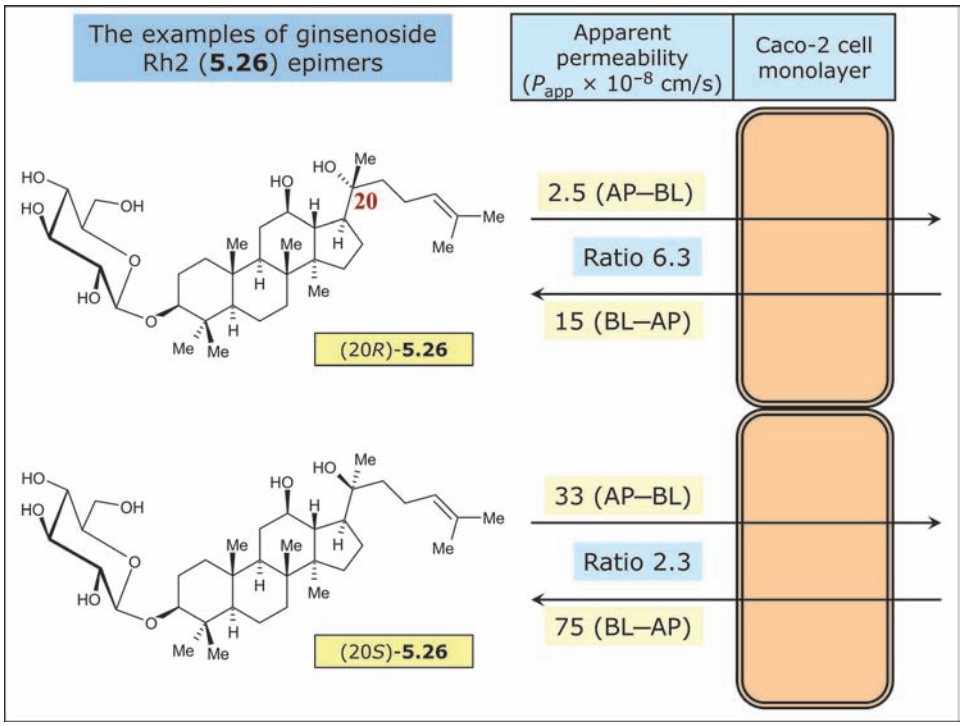

Fig. 5.33. *Ginsenoside Rh2* (**5.26**) is a steroidal saponin of the protopanaxadiol type whose many pharmacological effects have attracted much interest. Because its oral bioavailability is low, studies have been conducted to understand the underlying biological causes, the large size and high hydrophilicity of such compounds accounting for a *very low passive absorption*. A further variable in such studies was the fact that ginsenoside Rh2 exists as two epimers distinguished by their absolute configuration at C(20).

Investigations in *Caco-2 cell monolayers* (an *in vitro* model of intestinal absorption) showed the rate of cellular uptake to be low, with the (20*S*)-epimer penetrating at double the rate of the (20*R*)-epimer [157][158]. More detailed *transepithelial experiments* dealt with the *apparent permeability* (P_{app}) of the two epimers in both directions, namely from the *apical side* (AP, 'the *absorptive direction*') to the *basolateral side* (BS, 'the *secretory direction*'). The results are quite impressive, showing the influx (AP–BL) of the (20*R*)-epimer to be *ca.* 13 times slower than that of the (20*S*)-epimer, while its efflux (BL–AP) was only five times slower. These data point to marked stereoselectivities in the influx and efflux processes. Studies using inhibitors of P-gp and other *ABC transporters* revealed decreased efflux and increased absorptive permeability, confirming the involvement of such transporters in the secretory efflux process. In addition, evidence also indicated *ABC carrier-mediated influx transport* to be involved, although the balance favors the efflux processes as shown.

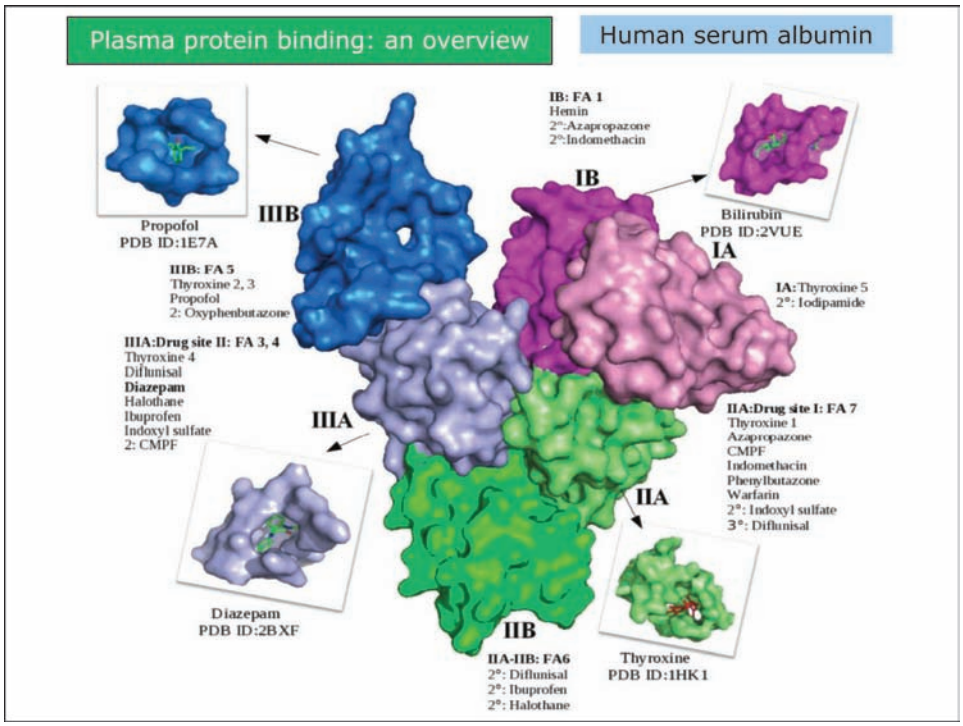

Fig. 5.34. The disposition of drugs in the body is influenced by their *reversible binding* to proteins and biomacromolecules other than those involved in their pharmacological action(s) or metabolism, a phenomenon that creates a '*drug reservoir*' and sometimes serves to prolong their duration of action. Such proteins exist in tissues and blood, but quantitatively the most important ones are those found in the *blood serum or plasma* [159–161].

Almost all drugs present in the systemic circulation are bound reversibly to one or more plasma proteins, most notably to *serum albumin*. In general, only the free fraction is available to exert the drug's effects, undergo metabolism or pass across cell membranes. However, since the free fraction is usually in facile equilibrium with the bound drug, this binding is seldom a major determinant of a drug's pharmacodynamic or pharmacokinetic profile.

Human serum albumin (HSA), the most abundant plasma protein (*ca.* 40 g/l, *ca.* 0.6 mM; 60% of plasma protein content) is highly soluble and negatively charged. It has a remarkable binding capacity for both endogenous and exogenous substances, including a wide range of drugs. This is due to the existence of several *binding domains*, as shown here (reproduced from [162] with permission). It has long been known that HSA possesses two specific drug binding sites, termed in the literature as *drug site I* (located in subdomain IIA) and *drug site II* (in subdomain IIIA). Site I ligands are principally bulky negatively charged heterocyclic compounds, while drug site II (also called the indole-benzodiazepine site) preferentially binds stick-like aromatic carboxylic acids with a negative charge clearly separated from the hydrophobic region of the molecule. However, these structural features do not distinguish the two sites, as many

ligands are known to bind to both sites, though with different affinities. Other minor drug binding sites are also apparent in the *Figure*.

X-Ray crystallography investigations have revealed that *drug site I* is a large, flexible, multi-chamber cavity with an entrance of *ca.* 10 Å in diameter. Ligands are bound in the pocket by hydrophobic contacts with lipophilic side chains within the site. In addition, appropriate ligands can form H-bonds with basic residues. Site I is very large and is not completely filled, allowing it to accommodate pairs of unrelated ligands simultaneously. In contrast, although both sites have largely nonpolar cavities, the cavity of *drug site II* is smaller and more rigid. Consequently, this site can show stereoselectivity in binding, *e.g.*, L-tryptophan shows a 100-fold higher HSA affinity than the D-enantiomer.

AAG (human α_1-acid glycoprotein, orosomucoid, also abbreviated as AGP) is another important macromolecule despite its comparatively low blood concentrations (0.6 – 1.2 mg/ml; 1 – 3% of plasma-protein content). It is a small acute-phase glycoprotein which *is negatively charged* at physiological pH and contains a large proportion of *carbohydrates* (40% by weight). AAG interacts with a variety of ligands. In particular, it is a high-affinity carrier for *most basic drugs* including β-blockers, antidepressants, neuroleptics, and local anaesthetics [160]. Structure–binding relations suggest that high-affinity ligands feature a privileged topographic pattern comprising a basic N-atom, a ring binding in a hydrophobic pocket, and another ring interacting with a hydrophobic area [163]. Such a pattern is compatible with enantioselective binding, as confirmed by the comparatively limited number of available data.

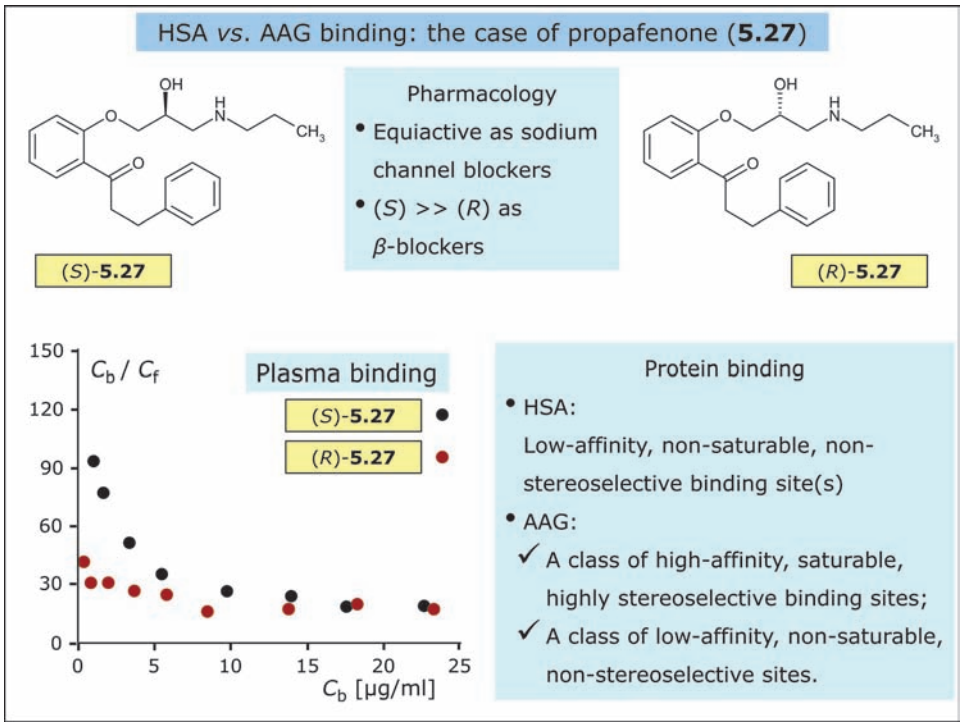

Fig. 5.35. There have been numerous reports on differences between the protein binding of the enantiomers of chiral drugs, but the differences are generally modest. Two comprehensive reviews [164][165] present data on the enantiomers of drugs from many pharmacological classes; for whole plasma and serum albumin, the binding ratio of the enantiomers is rarely if ever above 2. For a smaller number of drugs, data are also available on their binding to AAG, and here the enantiomer binding ratio is often greater, up to 7.

Further to their analysis of stereoselective transport (see above), *Leach et al.* [154] also looked at in-house data on the plasma protein binding of several hundred pairs of enantiomers in rat and human plasma. Their findings indicate a dependence on chirality of plasma protein binding in the plasma of both species. While plasma protein binding is in part a function of lipophilicity, the three-dimensional interaction between the compounds and the various binding sites on plasma proteins can also be important. It is interesting to note that they estimate the binding ratio between 95% of the pairs of enantiomers tested to be within 1 and 1.8, consistent with data reported in the review mentioned above [164].

Binding data obtained with blood plasma may be quite difficult to interpret, mainly due to sometimes overwhelming concentration effects. Comparing such data with binding to individual proteins (often HSA and AAG) may be quite enlightening, as illustrated here with the anti-arrhythmic drug *propafenone* (**5.27**) [166]. Some results from its binding in human plasma appear in the lower left part of the *Figure*, where C_b is the concentration of the bound drug, and C_f is the concentration of the free drug. The

plot reveals an enantioselectivity larger than twofold at the lowest concentrations, progressively decreasing to an (*R*)/(*S*) ratio of 1 at the highest concentrations.

Further experiments using human plasma proteins showed a modest, non-stereoselective and non-saturable binding to HAS, and two classes of binding sites on AAG, one whose behavior toward propafenone resembled that of HSA, and a second class of high-affinity, non-saturable, and enantioselective sites able to explain much of the drug's behavior in plasma.

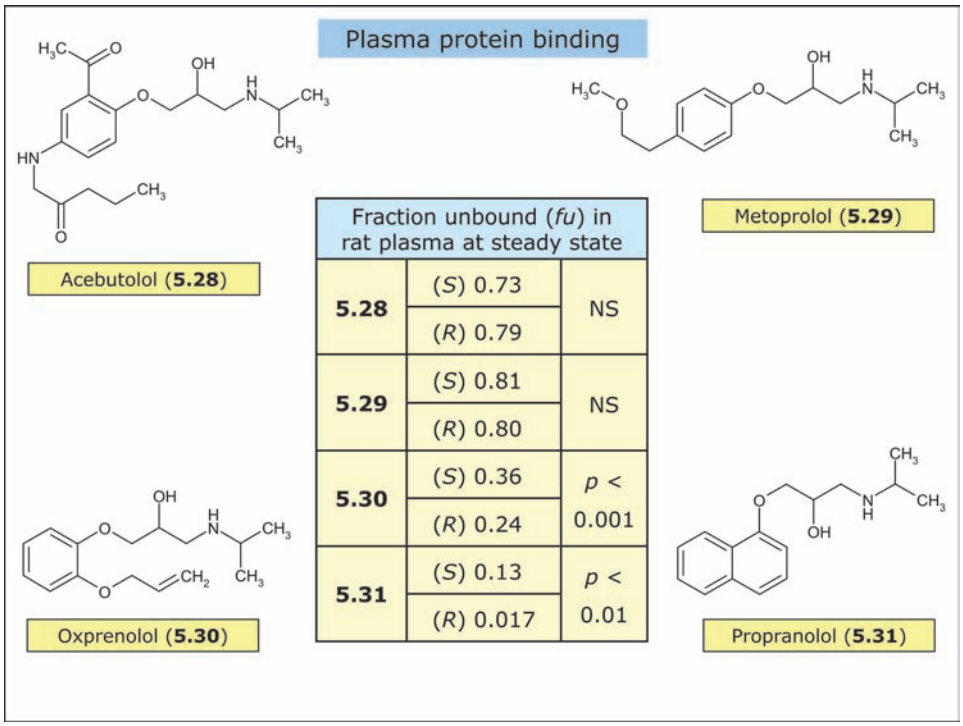

Fig. 5.36. In this *Figure*, we present some of the results from a large study on the binding and distribution of β-blockers [167]. The plasma binding of *acebutolol* (**5.28**) and *metoprolol* (**5.29**) as assessed by their unbound fraction (*fu*) was modest (NS, not significant), suggesting that no site on either HSA or AAG showed a high affinity toward these rather hydrophilic drugs. In contrast, *oxprenolol* (**5.30**) and *propranolol* (**5.31**), which are slightly and markedly more lipophilic, respectively, showed *higher binding affinities*. This was especially the case for propranolol, to which one can add that these affinities corresponded to a distinct (oxprenolol) and marked (propranolol) *enantioselectivity*. Several studies showed that the results with propranolol can be interpreted as were those with propafenone, namely that the enantioselectivity of its plasma protein binding is due to AAG (see the previous *Figure*) [168].

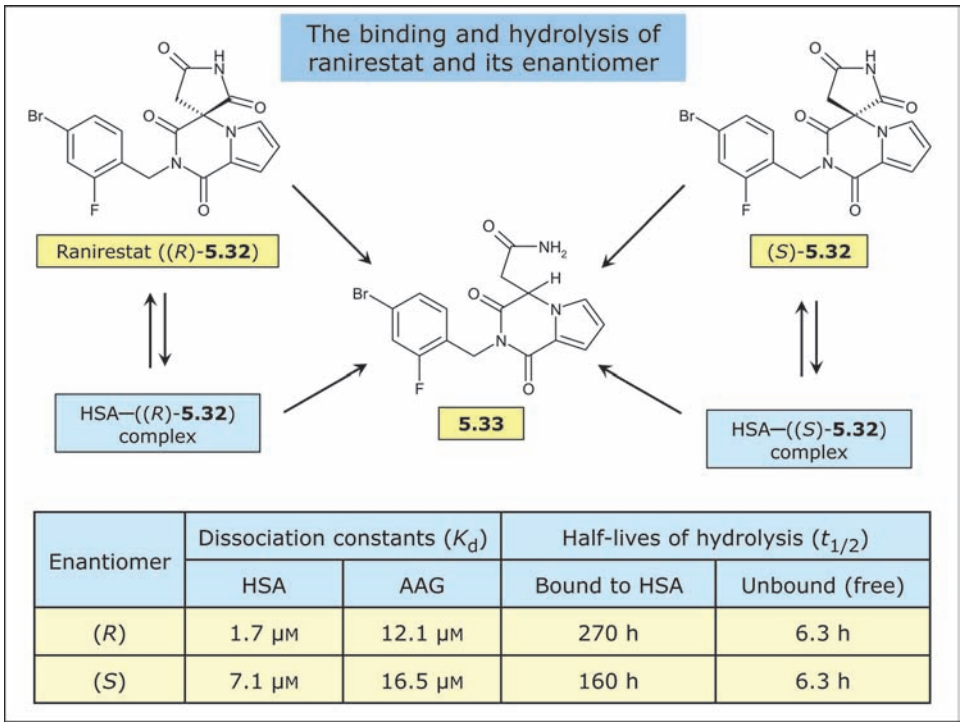

Enantiomer	Dissociation constants (K_d)		Half-lives of hydrolysis ($t_{1/2}$)	
	HSA	AAG	Bound to HSA	Unbound (free)
(*R*)	1.7 μM	12.1 μM	270 h	6.3 h
(*S*)	7.1 μM	16.5 μM	160 h	6.3 h

Fig. 5.37. Our last example is an intriguing one, as it deals with an unexpected and seldom observed consequence of plasma protein binding, namely protection against chemical degradation. *Ranirestat* (AS-3201; **5.32**) is a potent inhibitor of aldose reductase now in late clinical trials to delay or prevent secondary diabetic complications, in particular retinopathy and blindness. Ranirestat is the (−)-(*R*)-eutomer and an acidic compound due to deprotonation of its succinimide ring. The same ring is sensitive to *hydrolytic opening*, a reversible reaction rapidly followed by *irreversible decarboxylation to the inactive compound* **5.33** (probably produced in racemic form).

In an extensive investigation, the *plasma protein binding* and *stability* of the two enantiomers have been compared [169]. As shown, both isomers did bind to HSA and AAG, revealing that binding was stereoselective to both proteins but mainly toward the former. Indeed, the affinity of the (*R*)-isomer was about fourfold and 1.4-fold higher for HSA and AAG, respectively. Even more impressive was the *enantioselective protection against hydrolysis* caused by binding to HSA. While the half-lives of hydrolysis of the two unbound enantiomers were identical and rather fast at pH 7.4 and 25 °C, the stability of the (*R*)-eutomer was increased 43-fold when HSA-bound, and that of the (*S*)-distomer 25-fold, a difference of 1.7 times in favor of the eutomer.

REFERENCES

[1] 'Chirality in Drug Research', Eds. E. Francotte, W. Lindner, Wiley-VCH, Weinheim, Germany, 2006, 351 p.
[2] 'Stereochemical Aspects of Drug Action and Disposition', Eds. M. Eichelbaum, B. Testa, A. Somogyi, Eds, Springer Verlag, Berlin, 2003, 442 p.
[3] A. F. Casy, 'The Steric Factor in Medicinal Chemistry – Dissymmetric Probes of Pharmacological Receptors', Plenum Press, New York, 1993, 570 p.
[4] 'Biological Asymmetry and Handedness', Eds. G. R. Bock, J. Marsh, Ciba Foundation Symposium 162, John Wiley & Sons, Chichester, 1991, 327 p.
[5] 'Chirality and Biological Activity', Eds. B. Holmstedt, H. Frank, B. Testa, Liss, New York, 1990, 283 p.
[6] 'Problems and Wonders of Chiral Molecules', Ed. M. Simonyi, Akadémiai Kiadó, Budapest, 1990, 400 p.
[7] 'Stereoselectivity of Pesticides – Biological and Chemical Problems', Eds. E. J. Ariëns, J. J. S. van Rensen, W. Welling, Elsevier, Amsterdam, 1988, 544 p.
[8] 'Stereochemistry and Biological Activity of Drugs', Eds. E. J. Ariëns, W. Soudijn, P. B. M. Timmermans, Blackwell, Oxford, 1983, 194 p.
[9] 'Stereochemistry', Ed. C. Tamm, Elsevier, Amsterdam, 1982, 342 p.
[10] G. H. Wagnière, 'On Chirality and the Universal Asymmetry', Verlag Helvetica Chimica Acta, Zürich, and Wiley-VCH, Weinheim, 2007, 247 p.
[11] J. Gal, '*Carl Friedrich Naumann and the Introduction of Enantio Terminology: A Review and Analysis on the 150th Anniversary*', *Chirality* **2008**, *19*, 89 – 98.
[12] B. Testa, S. D. Krämer, '*The Biochemistry of Drug Metabolism – An Introduction – Part 1. Principles and Overview*', *Chem. Biodiversity* **2006**, *3*, 1053 – 1101; B. Testa, S. D. Krämer, 'The Biochemistry of Drug Metabolism: Principles, Redox Reactions, Hydrolyses', Verlag Helvetica Chimica Acta, Zürich, and Wiley-VCH, Weinhein, 2008, Vol. 1, 319 p.
[13] M. A. Piutti, '*Sur une nouvelle espèce d'asparagine*', *C. R. Hebd. Séances Acad. Sci.* **1886**, 134 – 138.
[14] M. Gardner, 'The Ambidextrous Universe', Penguin Books, New York, 1982, 293 p.
[15] A. R. Cushny, 'Biological Relations of Optically Isomeric Substances', Williams & Wilkins, Baltimore, 1926.
[16] C. L. Dodgson [Lewis Carroll], 'Through the Looking-Glass and What Alice Found There', Macmillan, London, 1871 (in 'The Penguin Complete Lewis Carroll', Penguin Books, London, 1982).
[17] J. M. Mayer, B. Testa, '*Chiral Recognition in Drug Metabolism and Disposition*', *Int. J. Bio-Chromatogr.* **2000**, *5*, 297 – 312.
[18] B. Testa, J. Mayer, '*Chiral Recognition in Biochemical Pharmacology: An Overview*', in 'Stereochemical Aspects of Drug Action and Disposition', Eds. M. Eichelbaum, B. Testa, A. Somogyi, Springer Verlag, Berlin, 2003, pp. 143 – 159.
[19] L. H. Easson, E. Stedman, '*Studies on the Relationship between Chemical Constitution and Physiological Action. V. Molecular Dissymmetry and Physiological Activity*', *Biochem. J.* **1933**, *27*, 1257 – 1266.
[20] A. R. Fersht, '*The Hydrogen Bond in Molecular Recognition*', *Trends Biochem. Sci.* **1987**, *12*, 301 – 304.
[21] V. R. Meyer, M. Rais, '*A Vivid Model of Chiral Recognition*', *Chirality* **1989**, *1*, 167 – 169.
[22] L. Salem, X. Chapuisat, G. Segal, P. C. Hiberty, C. Minot, C. Leforestier, P. Sautet, '*Chirality Forces*', *J. Am. Chem. Soc.* **1987**, *109*, 2887 – 2894.
[23] S. F. Mason, '*The Development of Concepts of Chiral Discrimination*', *Chirality* **1989**, *1*, 183 – 191.
[24] S. Topiol, M. Sabio, '*Elucidation of Chiral Recognition Principles*', *Enantiomer* **1996**, *1*, 251 – 265.
[25] T. D. Booth, D. Wahnon, I. W. Wainer, '*Is Chiral Recognition a Three-Point Process?*', *Chirality* **1997**, *9*, 96 – 98.
[26] V. A. Davankov, '*The Nature of Chiral Recognition: Is It a Three-Point Interaction*', *Chirality* **1997**, *9*, 99 – 102.

[27] R. Bentley, '*Diastereoisomerism, Contact Points, and Chiral Selectivity: a Four-Site Saga*', *Arch. Biochem. Biophys.* **2003**, *414*, 1 – 12.
[28] V. Sundaresan, R. Abrol, '*Biological Chiral Recognition: The Substate's Perspective*', *Chirality* **2005**, *17*, S30 – S39.
[29] A. D. Mesecar, D. E. Koshland Jr., '*A New Model for Protein Stereospecificity*', *Nature* **2000**, *403*, 614 – 615.
[30] P. J. Rice, A. Hamada, D. D. Miller, P. N. Patil, '*Asymmetric Catecholimidazolines and Catecholamidines: Affinity and Efficacy Relationships at the alpha Adrenoceptor in Rat Aorta*', *J. Pharmacol. Exp. Ther.* **1987**, *242*, 121 – 130; P. N. Patil, C. Li, V. Kumari, J. P. Hieble, '*Analysis of Efficacy of Chiral Adrenergic Agonists*', *Chirality* **2008**, *20*, 529 – 543.
[31] R. R. Ruffolo Jr., '*Chirality in α- and β-Adrenoceptor Agonists and Antagonists*', *Tetrahedron* **1991**, *48*, 9953 – 9980.
[32] P. Ciapetti, B. Ghiethlen, '*Molecular Variations Based on Isosteric Replacements*', in 'The Practice of Medicinal Chemistry', 3rd edn., Ed. C. G. Wermuth, Academic Press, London, 2008, pp. 290 – 342.
[33] R. R. Ruffolo Jr., '*Important Concepts of Receptor Theory*', *J. Autonom. Pharmacol.* **1982**, *2*, 277 – 295.
[34] B. Testa, '*Mechanisms of Chiral Recognition in Xenobiotic Metabolism and Drug-Receptor Interactions*', *Chirality* **1989**, *1*, 7 – 9.
[35] B. Testa, '*Mechanisms of Chiral Recognition in Pharmacology: The Easson–Stedman Model Revisited*', *Acta Pharm. Nord.* **1990**, *2*, 137 – 144.
[36] R. R. Ruffolo Jr., T. A. Spradlin, G. D. Pollock, J. E. Waddell, P. J. Murphy, '*Alpha and Beta Adrenergic Effects of the Stereoisomers of Dobutamine*', *J. Pharmacol. Exp. Ther.* **1981**, *219*, 447 – 452.
[37] B. Waldeck, '*The β_1-Selective Adrenoceptor Agonist Dobutamine: A Fallacy Being Perpetuated*', *Chirality* **2011**, *23*, 63 – 64.
[38] H. Fuder, B. Jung, '*Affinity and Efficacy of Racemic, (+)-, and (−)-Methacholine in Muscarinic Inhibition of [^{3}H]Noradrenaline Release*', *Br. J. Pharmacol.* **1985**, *84*, 477 – 487.
[39] http://en.wikipedia.org/wiki/Hermann_Emil_Fischer.
[40] D. E. Koshland Jr., '*Role of Flexibility in the Specificity, Control and Evolution of Enzymes*', *FEBS Lett.* **1976**, *62*, E47 – E52.
[41] D. E. Koshland Jr., '*The Key-Lock Theory and the Induced Fit Theory*', *Angew. Chem., Int. Ed.* **1994**, *33*, 2375 – 2378.
[42] C. B. Post, W. J. Ray Jr., '*Reexamination of Induced Fit as a Determinant of Substrate Specificity in Enzymatic Reactions*', *Biochemistry* **1995**, *34*, 15881 – 15885.
[43] K. A. Johnson, '*Role of Induced Fit in Enzyme Specificity: A Molecular Forward/Reverse Switch*', *J. Biol. Chem.* **2008**, *283*, 26297 – 26301.
[44] C. A. Sotriffer, '*Accounting for Induced-Fit Effects in Docking: What Is Possible and What Is Not?*', *Curr. Top. Med. Chem.* **2011**, *11*, 179 – 191.
[45] J. P. Changeux, S. Edelstein, '*Conformational Selection or Induced Fit? 50 Years of Debate Resolved*', *F1000 Biol. Rep.* **2011**, *3*, 19.
[46] D. Herschland, '*The Role of Induced Fit and Conformational Changes of Enzymes in Specificity and Catalysis*', *Bioorg. Chem.* **1988**, *16*, 62 – 96.
[47] T. Kenakin, '*Receptor Conformational Induction versus Selection: All Part of the Same Energy Landscape*', *Trends Pharmacol. Sci.* **1996**, *17*, 190 – 191; R. F. Bruns, '*Conformational Induction versus Conformational Selection: Evidence from Allosteric Enhancers*', *Trends Pharmacol. Sci.* **1996**, *17*, 189.
[48] G. G. Hammes, Y. C. Chang, T. G. Oas, '*Conformational Selection or Induced Fit: A Flux Description of Reaction Mechanism*', *Proc. Natl. Acad. Sci. U.S.A.* **2009**, *106*, 13737 – 13741.
[49] D. D. Boehr, R. Nussinov, P. E. Wright, '*The Role of Dynamic Conformational Ensembles in Biomolecular Recognition*', *Nat. Chem. Biol.* **2009**, *5*, 789 – 796.
[50] T. R. Weikl, C. Deuster, '*Selected-Fit versus Induced-Fit Protein Binding: Kinetic Differences and Mutational Analysis*', *Proteins* **2009**, *75*, 104 – 110.

[51] P. Csermely, R. Palotai, R. Nussimov, '*Induced Fit, Conformational Selection and Independent Dynamic Segments: An Extended View of Binding Events*', *Trends Biochem. Sci.* **2010**, *35*, 539 – 546.
[52] H. X. Zhou, '*From Induced Fit to Conformational Selection: A Continuum of Binding Mechanism Controlled by the Timescale of Conformational Transitions*', *Biophys. J.* **2010**, *98*, L15 – L17.
[53] D. A. Silva, G. R. Bowman, A. Sosa-Peinado, X. Huang, '*A Role for Both Conformational Selection and Induced Fit in Ligand Binding by the LAO Protein*', *PloS Comput. Biol.* **2011**, *7*(5), e1002054.
[54] H. X. Kondo, N. Okimoto, G. Morimoto, M. Taiji, '*Free Energy Landscapes of Protein Domain Movements upon Ligand Binding*', *J. Phys. Chem. B* **2011**, *115*, 7629 – 7636.
[55] G. Klebe, '*Mechanisms of Stereoselective Binding to Functional Proteins*', in 'Stereochemical Aspects of Drug Action and Disposition', Eds. M. Eichelbaum, B. Testa, A. Somogyi, Springer Verlag, Berlin, 2003, pp. 183 – 198.
[56] A. C. Kruse, J. Hu, A. C. Pan, D. H. Arlow, D. M. Rosenbaum, E. Rosemond, H. F. Green, T. Liu, P. S. Chae, R. O. Dror, D. E. Shaw, W. I. Weis, J. Wess, B. K. Kobilka, '*Structure and Dynamics of the M3 Muscarinic Acetylcholine Receptor*', *Nature* **2012**, *482*, 552 – 556; K. Haga, A. C. Kruse, H. Asada, T. Yurugi-Kobayashi, M. Shiroishi, C. Zhang, W. I. Weis, T. Okada, B. K. Kobilka, T. Haga, T. Kobayashi, '*Structure of the Human M2 Muscarinic Acetylcholine Receptor Bound to an Antagonist*', *Nature* **2012**, *482*, 547 – 551.
[57] A. Pedretti, G. Vistoli, C. Marconi, B. Testa, '*Muscarinic Receptors: A Comparative Analysis of Structural Features and Binding Modes through Homology Modelling and Molecular Docking*', *Chem. Biodiversity* **2006**, *3*, 481 – 501; A. Pedretti, G. Vistoli, B. Testa, R. Matucci, '*The Conformational and Property Space of Acetylcholine Bound to Muscarinic Receptors: An Entropy Component Accounts for the Subtype Selectivity of Acetylcholine*', *Arch. Biochem. Biophys.* **2007**, *464*, 112 – 121.
[58] G. Duncan, D. J. Collison, '*Role of the Non-Neuronal Cholinergic System in the Eye: A Review*', *Life Sci.* **2003**, *72*, 2013 – 2019.
[59] K. Cannard, '*The Acute Treatment of Nerve Agent Exposure*', *J. Neurol. Sci.* **2006**, *249*, 86 – 94.
[60] C. Ghelardini, F. Gualtieri, N. M. Romanelli, P. Angeli, G. Pepeu, G. M. Giovannini, F. Casamenti, P. Malmberg-Aiello, A. Giotti, A. Bartolini, '*Stereoselective Increase in Cholinergic Transmission by R-(+)-Hyoscyamine*', *Neuropharmacology* **1997**, *36*, 281 – 294.
[61] J. Singh, T. J. Hagen, '*Chirality and Biological Activity*', in 'Burger's Medicinal Chemistry, Drug Discovery, and Development', 7th edn., Eds. D. J. Abraham, D. P. Rotella, John Wiley & Sons, Hoboken, 2010, pp. 127 – 166.
[62] A. G. Draffan, G. R. Evans, J. A. Henshilwood, '*Chirality and Biological Activity*', in 'Burger's Medicinal Chemistry & Drug Discovery, 6th edn., Ed. D. J. Abraham, John Wiley & Sons, Hoboken, 2003, pp. 781 – 826.
[63] 'Chirality in Drug Design and Development', Eds. I. K. Reddy, R. Mehvar, Dekker, New York, 2004, 444 pages.
[64] W. Soudijn, I. van Wijngaarden, A. P. Ijzerman, '*Stereoselectivity of Drug-Receptor Interactions*', *IDrugs* **2003**, *6*, 43 – 56.
[65] W. Soudijn, I. van Wijngaarden, A. P. Ijzerman, '*Enantioselectivity in Drug-Receptor Interactions*', in 'Stereochemical Aspects of Drug Action and Disposition', Eds. M. Eichelbaum, B. Testa, A. Somogyi, Springer Verlag, Berlin, 2003, pp. 161 – 182.
[66] C. Valenzuela, '*Stereoselective Drug-Channel Interactions*', in 'Stereochemical Aspects of Drug Action and Disposition', Eds. M. Eichelbaum, B. Testa, A. Somogyi, Springer Verlag, Berlin, 2003, pp. 199 – 228.
[67] D. J. Triggle, '*Stereoselectivity of Drug Action*', *Drug Discovery Today* **1997**, *2*, 138 – 147; D. J. Triggle, '*The Stereoselectivity of Drug Action*', *Pharm. News* **2001**, *8*, 10 – 13.
[68] A. Brossi, '*Chiral Drugs: Synopsis*', *Med. Res. Rev.* **1994**, *14*, 665 – 691.
[69] B. Holmstedt, '*The Use of Enantiomers in Biological Studies: A Historical Review*', in 'Chirality and Biological Activity', Eds. B. Holmstedt, H. Frank, B. Testa, Liss, New York, 1990, pp. 1 – 14.
[70] M. Simonyi, '*On Chiral Drug Action*', *Med. Res. Rev.* **1984**, *4*, 359 – 413.
[71] P. S. Portoghese, '*Relationships between Stereostructure and Pharmacological Activities*', *Annu. Rev. Pharmacol.* **1970**, *10*, 51 – 76.

[72] A. H. Beckett, '*The Importance of Steric, Stereochemical and Physico-Organic Features in Drug Metabolism and Drug Action*', *Pure Appl. Chem.* **1969**, *19*, 231 – 248.
[73] A. H. Beckett, '*Stereochemical Factors in Biological Activity*', in 'Progress in Drug Research. Vol. 1', Ed. E. Jucker, Birkhäuser, Basel, 1959, pp. 455 – 530.
[74] C. D. Sieber, A. Hänsicke, T. Nagel, '*Stereochemical Comparison of Nebivolol with other β-Blockers*', *Chirality* **2008**, *20*, 103 – 109.
[75] K. E. Furse, T. P. Lybrand, '*Three-Dimensional Models for β-Adrenergic Receptor Complexes with Agonists and Antagonists*', *J. Med. Chem.* **2003**, *46*, 4450 – 4462.
[76] B. Waldeck, '*Chiral Aspects of β-Adrenergic Agonists*', *Pharm. News* **2001**, *8*, 25 – 31.
[77] N. El Tayar, B. Testa, H. van de Waterbeemd, P. A. Carrupt, A. J. Kaumann, '*Influence of Lipophilicity and Chirality on the Selectivity of Ligands for β_1- and β_2-Adrenoceptors*', *J. Pharm. Pharmacol.* **1988**, *40*, 609 – 612.
[78] R. T. Coutts, G. B. Baker, '*Implications of Chirality and Geometic Isomerism in Some Psychoactive Drugs and Their Metabolites*', *Chirality* **1989**, *1*, 99 – 120.
[79] D. J. Triggle, '*Ion Channels as Pharmacologic Receptors: The Chirality of Drug Interactions*', *Chirality* **1996**, *8*, 35 – 38; D. J. Triggle, '*On the Other Hand: The Stereoselectivity of Drug Action at Ion Channels*', *Chirality* **1994**, *6*, 58 – 62.
[80] S. Goldmann, J. Stoltefuss, '*1,4-Dihydropyridines – Effects of Chirality and Conformation on the Calcium Antagonists and Calcium Agonist Activities*', *Angew. Chem., Int. Ed.* **1991**, *30*, 1559 – 1578.
[81] E. J. Moody, '*Chirality and General Anesthetic Action*', *Pharm. News* **2001**, *8*, 36 – 41.
[82] N. P. Franks, W. R. Lieb, '*Molecular and Cellular Mechanisms of General Anaesthesia*', *Nature* **1994**, *367*, 607 – 614.
[83] J. Caldwell, B. Testa, '*Criteria for the Acceptability of Experimental Evidence for the Enantiomeric Composition of Xenobiotics and Their Metabolites*', *Drug Metab. Dispos.* **1987**, *15*, 587 – 588.
[84] R. B. Barlow, F. M. Franks, J. D. M. Pearson, '*The relation between biological activity and the degree of optical resolution of optical isomers*', *J. Pharm. Pharmacol.* **1972**, *24*, 753 – 761.
[85] J. Trofast, K. Österberg, B. L. Källström, B. Waldeck, '*Steric Aspects of Agonism and Antagonism at β-Adrenoceptors: Synthesis of and Pharmacological Experiments with the Enantiomers of Formoterol and Their Diastereomers*', *Chirality* **1991**, *3*, 443 – 450.
[86] B. Waldeck, '*Biological Significance of the Enantiomeric Purity of Drugs*', *Chirality* **1993**, *5*, 350 – 355.
[87] C. C. Pfeiffer, '*Optical Isomerism and Pharmacological Action, a Generalization*', *Science* **1956**, *124*, 29 – 31.
[88] R. Barlow, '*Enantiomers: How Valid is Pfeiffer's Rule?*', *Trends Pharmacol. Sci.* **1990**, *11*, 148 – 150.
[89] E. J. Ariëns, A. M. Simonis, '*Cholinergic and Anticholinergic Drugs, Do They Act on Common Receptors?*', *Ann. N.Y. Acad. Sci.* **1967**, *144*, 842 – 868.
[90] P. A. F. Lehmann, J. F. Rodrigues de Miranda, E. J. Ariëns, '*Stereoselectivity and Affinity in Molecular Pharmacology*', in 'Progress in Drug Research', Ed. E. Jucker, Birkhäuser, Basel, 1976, Vol. 20, pp. 101 – 129.
[91] P. A. F. Lehmann, '*Quantifying Stereoselectivity or How to Choose a Pair of Shoes when You Have Two Left Feet*', *Trends Pharmacol. Sci.* **1982**, *3*, 103 – 106; P. A. F. Lehmann, '*Stereoisomerism and Drug Action*', *Trends Pharmacol. Sci.* **1986**, *7*, 281 – 285.
[92] P. A. F. Lehmann, '*A Quantitative Stereo-Structure Activity Relationship Analysis of the Binding of Promiscuous Chiral Ligands to Different Receptors*', *Quant. Struct.-Act. Relat.* **1987**, *6*, 57 – 65.
[93] H. van de Waterbeemd, N. El Tayar, B. Testa, H. Wikström, B. Largent, '*Quantitative Structure-Activity Relationships and Eudismic Analyses of the Presynaptic Dopaminergic Activity and Dopamine D2 and Sigma Receptor Affinities of 3-(3-Hydroxyphenyl)-piperidines and Octahydrobenzo[f]quinolines*', *J. Med. Chem.* **1987**, *30*, 2175 – 2181.
[94] K. J. Romstedt, L. P. Lei, D. R. Feller, D. T. Witiak, F. Loiodice, V. Tortorella, '*Differential Eudismic Ratios in the Antagonism of Human Platelet Function by Phenoxy- and Thiophenoxyacetic Acids*', *Farmaco* **1996**, *51*, 107 – 114.
[95] K. Ding, J. Chen, M. Jin, X. Wu, J. Varady, C. Y. Yang, Y. Lu, J. R. Deschamps, B. Levant, S. Wang, '*Enantiomerically Pure Hexahydropyrazinoquinolines as Potent and Selective Dopamine 3 Subtype Receptor Ligands*', *J. Med. Chem.* **2005**, *48*, 3171 – 3181.

[96] J. P. Tillement, B. Testa, F. Brée, '*Compared Pharmacological Characteristics in Humans of Racemic Cetirizine and Levocetirizine, Two Histamine H_1-Receptor Antagonists*', *Biochem. Pharmacol.* **2003**, *66*, 1123 – 1126.

[97] M. Gillard, C. van der Perren, N. Moguilevsky, R. Massingham, P. Chatelain, '*Binding Characteristics of Cetirizine and Levocetirizine to Human H_1 Histamine Receptors: Contribution of Lys^{191} and Thr^{194}*', *Mol. Pharmacol.* **2002**, *61*, 391 – 399.

[98] A. D. Hughes, S. Hering, T. B. Bolton, '*Evidence That Agonist and Antagonist Enantiomers of the Dihydropyridine PN 202-791 Act at Different Sites on the Voltage-Dependent Calcium Channel of Vascular Muscle*', *Br. J. Pharmacol.* **1990**, *101*, 3 – 5.

[99] D. Conte Camerino, M. Mambrini, A. De Luca, D. Tricarico, S. H. Bryant, V. Tortorella, G. Bettoni, '*Enantiomers of Clofibric Acid Analogs Have Opposite Actions on Rat Skeletal Muscle Chloride Channels*', *Eur. J. Physiol.* **1988**, *413*, 105 – 107.

[100] A. De Luca, D. Tricarico, R. Wagner, S. H. Bryant, V. Tortorella, D. Conte Camerino, '*Opposite Effects of Enantiomers of Clofibric Acid Derivative on Rat Skeletal Muscle Chloride Conductance: Antagonism Studies and Theoretical Modeling of Two Different Receptor Site Interactions*', *J. Pharmacol. Exp. Ther.* **1992**, *260*, 364 – 368.

[101] B. Jiang, H. Wang, Q. M. Fu, Z. Y. Li, '*The Chiral Pyrethroid Cycloprothin: Stereoisomer Synthesis and Separation and Stereoselective Insecticidal Activity*', *Chirality* **2008**, *20*, 96 – 102.

[102] C. B. Eap, S. Crettol, J. S. Rougier, J. Schläpfer, L. Sintra Grilo, J. J. Déglon, J. Besson, M. Croquette-Krokar, P. A. Carrupt, H. Abriel, '*Stereoselective Block of hERG Channel by (*S*)-Methadone and QT Interval Prolongation in CYP2B6 Slow Metabolizers*', *Clin. Pharmacol. Ther.* **2007**, *81*, 719 – 728.

[103] H. Abriel, J. Schläpfer, D. I. Keller, B. Gavillet, T. Buclin, J. Biollaz, R. Stoller, L. Kappenberger, '*Molecular and Clinical Determinants of Drug-Induced Long QT Syndrome: A Iatrogenic Channelopathy*', *Swiss Med. Weekly* **2004**, *134*, 685 – 694.

[104] A. M. Aronov, '*In silico Models to Predict QT Prolongation*', in 'ADME-Tox Approaches', B. Testa, H. van de Waterbeemd, Eds., Vol. 5 in 'Comprehensive Medicinal Chemistry', 2nd edn, Eds. J. B. Taylor, D. J. Triggle, Elsevier, Oxford, 2007, pp. 933 – 954.

[105] N. Ansermot, O. Albayrak, J. Schläpfer, S. Crettol, M. Croquette-Krokar, M. Bourquin, J. J. Déglon, M. Faouzi, N. Scherbaum, C. B. Eap, '*Substitution of (*R,S*)-Methadone by (*R*)-Methadone*', *Arch. Internal Med.* **2010**, *170*, 529 – 536.

[106] I. N. Pessah, H. J. Lehmler, L. W. Robertson, C. F. Perez, E. Cabrales, D. D. Bose, W. Feng, '*Enantiomeric Specificity of (−)-2,2′,3,3′,6,6′-Hexachlorobiphenyl toward Ryanodine Receptor Types 1 and 2*', *Chem. Res. Toxicol.* **2008**, *22*, 201 – 207.

[107] R. A. Palmer, B. S. Potter, M. J. Leach, T. C. Jenkins, B. Z. Chowdhry, '*An Absolute Structure Template for a Unique Voltage-Gated Sodium Channel Binding Site*', *Med. Chem. Commun.* **2010**, *1*, 45 – 49.

[108] V. M. Vrudhula, B. Dasgupta, J. Qian-Cutrone, E. S. Kozlowski, C. G. Boissard, S. I. Dworetzky, D. Wu, Q. Gao, R. Kimura, V. K. Gribkoff, J. E. Starrett Jr., '*Atropisomeric 3-(β-hydroxyethyl)-4-arylquinolin-2-ones as Maxi-K Potassium Channel Openers*', *J. Med Chem.* **2007**, *50*, 1050 – 1057.

[109] Y. S. Zhou, L. K. Tay, D. Hughes, S. Donahue, '*Simulation of the Impact of Atropisomer Interconversion on Plasma Exposure of Atropisomers of an Endothelin Receptor Antagonist*', *J. Clin. Pharmacol.* **2004**, *44*, 680 – 688.

[110] B. Testa, S. D. Krämer, '*The Biochemistry of Drug Metabolism – An Introduction. Part 5: Metabolism and Bioactivity*', *Chem. Biodiversity* **2009**, *6*, 591 – 684; B. Testa, S. D. Krämer, 'The Biochemistry of Drug Metabolism: Conjugations, Consequences of Metabolism, Influencing Factors', Verlag Helvetica Chimica Acta, Zürich, and Wiley-VCH, Weinhein, 2010, 588 p.

[111] T. J. Edkins, M. Fronheiser, D. R. Bobbitt, J. E. Mills, T. M. Rossi, '*Enantiomeric Quantitation without Separation of Tramadol via Laser-Based Polarimetry*', *Enantiomer* **1996**, *1*, 97 – 107.

[112] R. B. Raffa, E. Friderichs, W. Reimann, R. P. Shank, E. E. Codd, J. L. Vaught, H. I. Jacoby, N. Selve, '*Complementary and Synergistic Antinociceptive Interaction between the Enantiomers of Tramadol*', *J. Pharmacol. Exp. Ther.* **1993**, *267*, 331 – 340.

[113] L. J. Scott, C. M. Perry, '*Tramadol. A Review of Its Use in Perioperative Pain*', *Drugs* **2000**, *60*, 139 – 176.

[114] M. Valle, M. J. Garrido, J. M. Pavón, R. Calvo, I. F. Trocóniz, '*Pharmacokinetic-Pharmacodynamic Modeling of the Antinocipeptive Effects of Main Active Metabolites of Tramadol, (+)-O-Desmethyltramadol and (−)-Desmethyltramadol, in Rats*', *J. Pharmacol. Exp. Ther.* **2000**, *293*, 646 – 653.

[115] S. Grond, T. Meuser, H. Uragg, H. J. Stahlberg, K. A. Lehmann, '*Serum Concentrations of Tramadol Enantiomers during Patient-Controlled Analgesia*', *Br. J. Clin. Pharmacol.* **1999**, *48*, 254 – 257.

[116] J. M. Mayer, B. Testa, '*Pharmacodynamics, Pharmacokinetics and Toxicity of Ibuprofen Enantiomers*', *Drugs Future* **1997**, *22*, 1347 – 1366.

[117] I. Tegeder, K. Williams, G. Geisslinger, '*Metabolic Chiral Inversion of 2-Arylpropionic Acids*', in 'Stereochemical Aspects of Drug Action and Disposition', Eds. M. Eichelbaum, B. Testa, A. Somogyi, Springer Verlag, Berlin, 2003, pp. 341 – 354.

[118] J. M. Mayer, M. Roy-de Vos, C. Audergon, B. Testa, '*Interactions between the in vitro Metabolism of Xenobiotics and Fatty Acids. The Case of Ibuprofen and Other Chiral Profens*', *Arch. Toxicol.* **1995**, *Suppl. 17*, 499 – 513.

[119] H. Hao, G. Wang, J. Sun, '*Enantioselective Pharmacokinetics of Ibuprofen and Involved Mechanisms*', *Drug Metab. Rev.* **2005**, *37*, 215 – 234.

[120] K. M. Knights, C. J. Drogemuller, '*Xenobiotic-CoA Ligases: Kinetic and Molecular Characterization*', *Curr. Drug Metab.* **2000**, *1*, 49 – 66; K. M. Knights, '*Role of Hepatic Fatty Acid:Coenzyme A Ligases in the Metabolism of Xenobiotic Carboxylic Acids*', *Clin. Exp. Pharmacol. Physiol.* **1998**, *25*, 776 – 782.

[121] R. Brugger, C. Reichel, B. Garcia Alia, K. Brune, T. Yamamoto, I. Tegeder, G. Geisslinger, '*Expression of Rat Liver Long-Chain Acyl-CoA Synthetase and Characterization of Its Role in the Metabolism of R-Ibuprofen and other Fatty Acid-Like Xenobiotics*', *Biochem. Pharmacol.* **2001**, *61*, 651 – 656.

[122] M. D. Lloyd, D. J. Darley, A. S. Wierzbicki, M. D. Threadgill, '*Alpha-Methylacyl-CoA Racemase – an 'Obscure' Metabolic Enzyme Takes Centre Stage*', *FEBS J.* **2008**, *275*, 1089 – 1102.

[123] W. Neupert, R. Brugger, C. Euchenhofer, K. Brune, G. Geisslinger, '*Effects of Ibuprofen Enantiomers and Its Coenzyme A Thioesters on Human Prostaglandin Endoperoxide Synthases*', *Br. J. Pharmacol.* **1997**, *122*, 487 – 492.

[124] N. Levoin, C. Blondeau, C. Guillaume, L. Grandcolas, F. Chrétien, J.-Y. Jouzeau, E. Benoit, Y. Chapleur, P. Netter, F. Lapicque, '*Elucidation of the Mechanism of Inhibition of Cyclooxygenases by Acyl-CoA and Acyl Glucuronide Conjugates of Ketoprofen*', *Biochem. Pharmacol.* **2004**, *68*, 1957 – 1969.

[125] 'Drug Bioavailability – Estimation of Solubility, Permeability, Absorption and Bioavailability', 2nd edn., Eds. H. van de Waterbeemd, B. Testa, Wiley-VCH, Weinheim, 2008, 624 p.

[126] 'ADME-Tox Approaches', Eds. B. Testa, H. van de Waterbeemd, Vol. 5 in 'Comprehensive Medicinal Chemistry', 2nd edn., Eds. J. B. Taylor, D. J. Triggle, Elsevier, Oxford, 2007.

[127] H. van de Waterbeemd, B. Testa, '*The Why and How of Absorption, Distribution, Metabolism, Excretion and Toxicity Research*', in 'ADME-Tox Approaches', Eds. B. Testa, H. van de Waterbeemd, Vol. 5 in 'Comprehensive Medicinal Chemistry', 2nd edn., Eds. J. B. Taylor, D. J. Triggle, Elsevier, Oxford, 2007, pp. 1 – 9.

[128] D. R. Brocks, '*Drug Disposition in Three Dimensions: An Update on Stereoselectivity in Pharmacokinetics*', *Biopharm. Drug Dispos.* **2006**, *27*, 387 – 406.

[129] G. T. Tucker, M. S. Lennard, '*Enantiomer Specific Pharmacokinetics*', *Pharmacol. Ther.* **1990**, *45*, 309 – 329.

[130] R. Mehvar, D. R. Brocks, M. Vakily, '*Impact of Stereoselectivity on the Pharmacokinetics and Pharmacodynamics of Antiarrhythmic Drugs*', *Clin. Pharmacokinet.* **2002**, *41*, 533 – 558.

[131] R. R. Shah, '*Improving Clinical Risk/Benefit through Stereochemistry*', in 'Stereochemical Aspects of Drug Action and Disposition', Eds. M. Eichelbaum, B. Testa, A. Somogyi, Springer Verlag, Berlin, 2003, pp. 401 – 432.

[132] K. Arimori, K. Yasuda, H. Katsuki, M. Nakano, '*Pharmacokinetic Differences between Lansoprazole Enantiomers in Rats*', *J. Pharm. Pharmacol.* **1998**, *50*, 1241 – 1245.

[133] P. M. Cerqueira, E. J. Cesarino, F. H. Mateus, Y. Mere Jr., S. R. Cavani, V. L. Lanchote, '*Enantioslectivity in the Steady-State Pharmacokinetics of Metoprolol in Hypertensive Patients*', *Chirality* **1999**, *11*, 591 – 597.

[134] J. Guan, J. Yang, J. Li, F. Li, '*Determination of Tenatoprazole Enantiomers and Their Enantioselective Pharmacokinetics in Rats*', *Chirality* **2009**, *21*, 613 – 618.

[135] A. L. Pardo, C. Godoy, C. C. Parisi, M. P. Marques, E. B. Coelho, V. L. Lanchote, '*Enantioselective Determination of Mexiletine and Its Metabolites p-Hydroxymexiletine and Hydroxymethylmexiletine in Rat Plasma by Normal-Phase LC-Tandem MS: Application to Pharmacokinetics*', *Chirality* **2009**, *21*, 648 – 656.

[136] M. Miura, T. Uno, M. Takeishi, T. Suzuki, '*Pharmacokinetics of Fexofenadine Enantiomers in Healthy Subjects*', *Chirality* **2007**, *19*, 223 – 227.

[137] Y. Akamine, M. Miura, S. Sunagawa, H. Kagaya, N. Yasui-Furukori, T. Uno, '*Influence of Drug-Transporter Polymorphisms on the Pharmacokinetics of Fexofenadine Enantiomers*', *Xenobiotica* **2010**, *40*, 782 – 789.

[138] U. Fagerholm, '*The Role of Permeability in Drug ADME/PK, Interactions and Toxicity, and the Permeability-Based Classification Systems (PCS)*', in 'Burger's Medicinal Chemistry, Drug Discovery, and Development', 7th edn., Eds. D. J. Abraham, D. P. Rotella, John Wiley & Sons, Hoboken, 2010, pp. 367 – 379.

[139] P. Artursson, S. Neuhoff, P. Matsson, S. Tavelin, '*Passive Permeability and Active Transport Models for the Prediction of Oral Absorption*', in 'ADME-Tox Approaches', Eds. B. Testa, H. van de Waterbeemd, Vol. 5 in 'Comprehensive Medicinal Chemistry', 2nd edn., Eds. J. B. Taylor, D. J. Triggle, Elsevier, Oxford, 2007, pp. 259 – 278.

[140] C. M. Head, K. R. Brain, '*Does Solute Stereochemistry Influence Percutaneous Penetration?*', *Chirality* **1995**, *7*, 305 – 309.

[141] W. Jäger, M. Mayer, G. Reznicek, G. Buchbauer, '*Percutaneous Absorption of the Monoterpene Carvone: Implication of Stereoselective Metabolism on Blood Levels*', *J. Pharm. Pharmacol.* **2001**, *53*, 637 – 642.

[142] A. Pagliara, P. A. Carrupt, G. Caron, P. Gaillard, B. Testa, '*Lipophilicity Profiles of Ampholytes*', *Chem. Rev.* **1997**, *97*, 3385 – 3400.

[143] R. S. Tsai, P. A. Carrupt, B. Testa, N. El Tayar, G. L. Grunewald, A. F. Casy, '*Influence of Stereochemical Factors on the Partition Coefficient of Diastereomers in a Biphasic Octan-1-ol/Water System*', *J. Chem. Res. (S)* **1993**, 298 – 299, *J. Chem. Res. (M)* **1993**, 1901 – 1920.

[144] J. M. Scherrmann, '*The Biology and Function of Transporters*', in 'ADME-Tox Approaches', Eds. B. Testa, H. van de Waterbeemd, Vol. 5 in 'Comprehensive Medicinal Chemistry', 2nd edn., Eds. J. B. Taylor, D. J. Triggle, Elsevier, Oxford, 2007, pp. 51 – 85.

[145] P. Anderle, C. U. Nielsen, '*Transporters in the Gastrointestinal Tract*', in 'Drug Bioavailability – Estimation of Solubility, Permeability, Absorption and Bioavailability', 2nd edn., Eds. H. van de Waterbeemd, B. Testa, Wiley-VCH, Weinheim, 2008, pp. 223 – 276; H. Spahn-Langguth, C. Dressler, C. Leisen, '*Intestinal Drug Transport: Stereochemical Aspects*', in 'Stereochemical Aspects of Drug Action and Disposition', Eds. M. Eichelbaum, B. Testa, A. Somogyi, Springer Verlag, Berlin, 2003, pp. 251 – 288.

[146] K. Maeda, H. Suzuki, Y. Sugiyama, '*Hepatic Transport*', in 'Drug Bioavailability – Estimation of Solubility, Permeability, Absorption and Bioavailability', 2nd edn., Eds. H. van de Waterbeemd, B. Testa, Wiley-VCH, Weinheim, 2008, pp. 277 – 332.

[147] K. M. Giacomini, S.-M. Huang, D. J. Tweedie and The International Transporter Consortium, '*Membrane Transporters in Drug Development*', *Nat. Rev. Drug Discovery* **2010**, *9*, 215 – 236.

[148] S. G. Aller, J. Yu, A. Ward, Y. Weng, S. Chittaboina, R. Zhuo, P. M. Harrell, Y. T. Trinh, Q. Zhang, I. L. Urbatsch, G. Chang, '*Structure of P-Glycoprotein Reveals a Molecular Basis for Poly-Specific Drug Binding*', *Science* **2009**, *323*, 1718 – 1722.

[149] F. Stoll, A. H. Göller, A. Hillisch, '*Utility of Protein Structures in Overcoming ADMET-Related Issues of Drug-Like Compounds*', *Drug Discovery Today* **2011**, *16*, 530 – 538.

[150] J.-P. Becker, G. Depret, F. Van Bambeke, P. M. Tulkens, M. Prévost, '*Molecular Models of Human P-Glycoprotein in Two Different Catalytic States*', *BMC Struct. Biol.* **2009**, doi:10.1186/1472-6807-9-3.

[151] E. Dolghih, C. Bryant, A. R. Renslo, M. P. Jacobson, '*Predicting Binding to P-Glycoprotein by Flexible Receptor Docking*', *PLoS Comput. Biol.* **2011**, *7*(6), e1002083.
[152] C. M. Brett, R. J. Orr, K. M. Giacomini, '*Stereoselective Renal Elimination*', in 'Stereochemical Aspects of Drug Action and Disposition', Eds. M. Eichelbaum, B. Testa, A. Somogyi, Springer Verlag, Berlin, 2003, pp. 355 – 375.
[153] E. Choong, M. Dobrinas, P. A. Carrupt, C. B. Eap, '*The Permeability P-Glycoprotein: A Focus on Enantioselectivity and Brain Distribution*', *Exp. Opin. Drug Metab. Toxicol.* **2010**, *6*, 953 – 965.
[154] A. G. Leach, E. A. Pilling, A. A. Rabow, S. Tomasi, N. Asaad, N. J. Buurma, A. Ballard, S. Narduolo, '*Enantiomeric Pairs Reveal that Key Medicinal Chemistry Parameters vary more than Simple Physical Property Based Models Can Explain*', *Med. Chem. Commun.* **2012**, *3*, 528 – 540.
[155] S. Crettol, P. Digon, K. Powell Golay, M. Brawand, C. B. Eap, '*In vitro P-Glycoprotein-Mediated Transport of (*R*)-, (*S*)-, (*R,S*)-Methadone, LAAM and Their Main Metabolites*', *Pharmacology* **2007**, *80*, 304 – 311.
[156] S. Baudry, Y. T. Pham, B. Baune, S. Vidrequin, C. Crevoisier, F. Gimenez, R. Farinotti, '*Stereoselective Passage of Mefloquine through the Blood-Brain Barrier in the Rat*', *J. Pharm. Pharmacol.* **1997**, *49*, 1086 – 1090.
[157] Y. Gu, G. J. Wang, X. L. Wu, Y. T. Zheng, J. W. Zhang, H. Ai, J. G. Sun, Y. W. Jia, '*Intestinal Absorption Mechanisms of Ginsenoside Rh2: Stereoselectivity and Involvement of ABC Transporters*', *Xenobiotica* **2010**, *40*, 602 – 612.
[158] J. Zhang, F. Zhou, F. Niu, M. Lu, X. Wu, J. Sun, G. Wang, '*Stereoselective Regulations of P-Glycoprotein by Ginsenoside Rh2 Epimers and the Potential Mechanisms from the View of Pharmacokinetics*', *PLoS One* **2012**, *7(4)*, e35768.
[159] P. Barton, R. P. Austin, R. E. Fessey, '*In vitro Models for Plasma Binding and Tissue Storage*', in 'ADME-Tox Approaches', Eds. B. Testa, H. van de Waterbeemd, Vol. 5 in 'Comprehensive Medicinal Chemistry', 2nd edn., Eds. J. B. Taylor, D. J. Triggle, Elsevier, Oxford, 2007, pp. 321 – 340.
[160] J. P. Tillement, G. Houin, R. Zini, S. Urien, E. Albengres, J. Barré, M. Lecomte, P. D'Athis, B. Sébille, '*The Binding of Drug to Blood Plasma Macromolecules: Recent Advances and Therapeutic Significance*', in 'Advances in Drug Research', Ed. B. Testa, Academic Press, London, 1984, Vol. 13, pp. 59 – 94.
[161] B. Fichtl, A. von Nieciecki, K. Walter, '*Tissue Binding versus Plasma Binding of Drugs: General Principles and Pharmacokinetic Consequences*', in 'Advances in Drug Research. Vol. 20', Ed. B. Testa, Academic Press, London, 1991, pp. 117 – 166.
[162] A. Varshney, P. Sen, E. Ahmad, M. Rehan, N. Subbarao, R. H. Khan, '*Ligand Binding Strategies of Human Serum Albumin: How Can the Cargo Be Utilized?*', *Chirality* **2010**, *22*, 77 – 87.
[163] F. Hervé, G. Caron, J. C. Duché, P. Gaillard, N. Abd. Rahman, A. Tsantili-Kakoulidou, P. A. Carrupt, P. d'Athis, J. P. Tillement, B. Testa, '*Ligand Specificity of the Genetic Variants of Human alpha-1-Acid Glycoprotein. Generation of a 3D-QSAR Model for Drug Binding to the A Variant*', *Mol. Pharmacol.* **1998**, *54*, 129 – 138.
[164] L. Escuder-Gilabert, M. A. Martínez-Gómez, R. M. Villanueva-Camañas, S. Sagrado, M. J. Medina-Hernández, '*Microseparation Techniques for the Study of the Enantioselectivity of Drug-Plasma Protein Binding*', *Biomed. Chromatogr.* **2009**, *23*, 225 – 238.
[165] P. J. Hayball, D. Mauleón, '*Enantioselective Plasma and Tissue Binding*', in 'Stereochemical Aspects of Drug Action and Disposition', Eds. M. Eichelbaum, B. Testa, A. Somogyi, Springer Verlag, Berlin, 2003, pp. 289 – 311.
[166] Y. Hong, Y. Tang, S. Zeng, '*Enantioselective Plasma Protein Binding of Propafenone: Mechanism, Drug Interaction, and Species Differences*', *Chirality* **2009**, *21*, 692 – 698.
[167] T. Rodgers, D. Leahy, M. Rowland, '*Tissue Distribution of Basic Drugs: Accounting for Enantiomeric, Compound and Regional Differences among β-Blocking Drugs in Rat*', *J. Pharm. Sci.* **2005**, *94*, 1237 – 1248.
[168] R. Pérez-Ruiz, R. Alonso, E. Nuin, I. Andreu, M. C. Jiménez, M. A. Miranda, '*Naphthalene Triplet Excited State as a Probe for the Assessment of Drug Distribution in Binary Protein Systems*', *J. Phys. Chem. B* **2011**, *115*, 4460 – 4468; Y. Ding, X. Zhu, B. Lin, '*Study of Interaction between Drug Enantiomers and Serum Albumin by Capillary Electrophoresis*', *Electrophoresis* **1999**, *20*, 1890 –

1894; G. Sager, R. Jaeger, C. Little, '*Binding of Prazosin and Propranolol at Variable alpha 1-Acid Glycoprotein and Albumin Concentrations*', *Br. J. Clin. Pharmacol.* **1989**, *27*, 229 – 234.

[169] M. Kurono, A. Fujii, M. Murata, B. Fujitani, T. Negoro, '*Stereospecific Recognition of a Spirosuccinimide Type Aldose Reductase Inhibitor (AS-3201) by Plasma Proteins: A Significant Role of Specific Binding by Serum Albumin in the Improved Potency and Stability*', *Biochem. Pharmacol.* **2006**, *71*, 338 – 353.

Received August 14, 2012